The NAC Transcription Factors OsNAC20 and OsNAC26 Regulate Starch and Storage Protein Synthesis[1][OPEN]

Juan Wang,[a,b,2] Zichun Chen,[a,b,2] Qing Zhang,[a,b] Shanshan Meng,[a,b] and Cunxu Wei[a,b,3,4]

[a]Jiangsu Provincial Key Laboratory of Crop Genetics and Physiology/Jiangsu Provincial Key Laboratory of Crop Genomics and Molecular Breeding, Yangzhou University, Yangzhou 225009, China
[b]Co-Innovation Center for Modern Production Technology of Grain Crops of Jiangsu Province/Joint International Research Laboratory of Agriculture and Agri-Product Safety of the Ministry of Education, Yangzhou University, Yangzhou 225009, China

ORCID IDs: 0000-0002-0079-9532 (J.W.); 0000-0002-2592-3843 (C.W.).

Starch and storage proteins determine the weight and quality of cereal grains. Synthesis of these two grain components has been comprehensively investigated, but the transcription factors responsible for their regulation remain largely unknown. In this study, we investigated the roles of NAM, ATAF, and CUC (NAC) transcription factors, OsNAC20, and OsNAC26 in starch and storage protein synthesis in rice (*Oryza sativa*) endosperm. OsNAC20 and OsNAC26 showed high levels of amino acid sequence similarity. Both were localized in the aleurone layer, starchy endosperm, and embryo. Mutation of *OsNAC20* or *OsNAC26* alone had no effect on the grain, while the *osnac20/26* double mutant had significantly decreased starch and storage protein content. OsNAC20 and OsNAC26 alone could directly transactivate the expression of *starch synthaseI* (*SSI*), *pullulanase* (*Pul*), *glutelin A1* (*GluA1*), *glutelin B4/5* (*GluB4/5*), *α-globulin*, and *16 kD prolamin* and indirectly influenced *plastidial disproportionating enzyme1* (*DPE1*) expression to regulate starch and storage protein synthesis. Although they could also bind to the promoters of *ADP-Glc pyrophosphorylase small subunit 2b* (*AGPS2b*), *ADP-Glc pyrophosphorylase large subunit 2* (*AGPL2*), and *starch branching enzymeI* (*SBEI*), and the expression of the three genes was largely decreased in the *osnac20/26* mutant, ADP-Glc pyrophosphorylase and starch branching enzyme activities were unchanged in this double mutant. In addition, OsNAC20 and OsNAC26 are main regulators of *Pul*, *GluB4*, *α-globulin*, and *16 kD prolamin*. In conclusion, OsNAC20 and OsNAC26 play an essential and redundant role in the regulation of starch and storage protein synthesis.

Rice (*Oryza sativa*) is one of the most important staple foods worldwide. Its endosperm is composed of ~80% starch and 10% storage protein. Starch is the main dietary source of energy, and protein plays an important role in the quality of rice grains. Therefore, revealing the basis of the regulation underlying starch and storage protein accumulation is essential for improvement of rice grain quality.

Although starch is a simple combination of Glc molecules, its biosynthesis in plant endosperm involves a series of complex and coordinated enzymatic actions. In the first step, ADP-Glc pyrophosphorylase (AGPase) converts Glc-1-phosphate into ADP-Glc, the substrate of starch synthesis (Beckles et al., 2001). Starch phosphorylase1 (Pho1) plays a critical role in starch initiation by extending the chain length of the initial primer (Satoh et al., 2008). Granule-bound starch synthaseI (GBSSI)/Waxy (Wx) produces amylose (Denyer et al., 2001). Amylopectin synthesis is mainly controlled by three types of biosynthetic enzymes, starch synthases (SSs), starch branching enzymes (SBEs), and debranching enzymes (DBEs; Nakamura, 2002; Davis et al., 2003; Tetlow, 2006). SSs and SBEs contribute to the extension of glucan chains and the formation of branch points, respectively. DBEs trim the irregular glucan structure created by SSs and SBEs to obtain ordered amylopectin branch chains. In addition, plastidial disproportionating enzyme1 (DPE1) has also been reported to take part in starch synthesis by transferring maltooligosyl groups from amylose and amylopectin to amylopectin (Dong et al., 2015).

Only a few regulators have been reported to participate in the regulation of starch synthesis, and most of these reports focus on rice and maize (*Zea mays*). Rice YB1 directly binds to the G-box of the *Wx* promoter and activates *Wx* transcription (Bello et al., 2019). Maize ZmEREB156 positively modulates *ZmSSIIIa* through

[1]This work was supported by the National Natural Science Foundation of China (grant no. 31800269), the Talent Project of Yangzhou University, and the Priority Academic Program Development of Jiangsu Higher Education Institutions.

[2]These authors contributed equally to the article.

[3]Author for contact: cxwei@yzu.edu.cn.

[4]Senior author.

The author responsible for distribution of materials integral to the findings presented in this article in accordance with the policy described in the Instructions for Authors (www.plantphysiol.org) is: Cunxu Wei (cxwei@yzu.edu.cn).

J.W. and C.W. conceived the project and designed the experiments; J.W., Z.C., Q.Z., and S.M. carried out all of the experiments; J.W., Z.C., and C.W. analyzed data and wrote the article; and all authors approved the article for publication.

[OPEN]Articles can be viewed without a subscription.

www.plantphysiol.org/cgi/doi/10.1104/pp.20.00984

the synergistic effect of Suc and abscisic acid (ABA; Huang et al., 2016; Li et al., 2018b). *ZmbZIP91* is homologous to *AtVIP1* and complements the altered starch phenotype of the *vip1* mutant in Arabidopsis (*Arabidopsis thaliana*) leaves. Further analyses indicate that ZmZIP91 directly binds to the promoters of the starch synthesis-related genes *AGPS1*, *SSI*, *SSIIIa*, and *ISA1* (Chen et al., 2016). In addition, OsbZIP33 has also been inferred to play a role in regulation of starch synthesis, as it is able to interact with the ACGT element buried in the promoter of *SBEI* and *Wx* (Cai et al., 2002). Recently, Song et al. (2020) reported that TubZIP28 in *Triticum urartu* and its homolog, TabZIP28 from common wheat (*Triticum aestivum*), play a role in the regulation of starch synthesis as TubZIP28 binds to the promoter of cytosolic AGPase and enhances its transcription and activity. Apart from the above-mentioned regulators that directly bind to the promoters of starch synthesis-related genes to regulate their expression, some other regulators such as ZmaNAC36, ZmNAC34, rice starch regulator1 (RSR1), disulfide isomerase1-2 protein (TaPDIL1-2), ZmMADS1a, and G protein γ-subunit DEP1/qPE9-1 also have an indirect or unknown role in the regulation of starch synthesis (Fu and Xue, 2010; Zhang et al., 2014, 2019a; Dong et al., 2019a, 2019b; Peng et al., 2019).

The major storage proteins in rice endosperm include acid- and alkaline-soluble glutelins, alcohol-soluble prolamins, and saline-soluble α-globulin. They comprise ~70%, 20%, and 3% of the total storage proteins, respectively (He et al., 2013). Based on their sequence similarity, glutelin genes are classified into four subfamilies, designated as *GluA*, *GluB*, *GluC*, and *GluD*. Prolamin genes are divided into three families, designated as *10 kD*, *13 kD*, and *16 kD*. The *GluA*, *GluB*, *10 kD*, and *13 kD* subfamilies are composed of several members (Saito et al., 2012; He et al., 2013).

Cis-regulatory elements, such as O2/O2-like and prolamin boxes, have been widely detected in the storage protein synthesis-related genes in cereal crops (Washida et al., 1999; Wu et al., 2000). Maize O2 directly binds to the O2 box to modulate almost all zein genes, except for genes encoding 16-kD γ- and 18-kD δ-zein, whereas O2 displays different activation activity for different zein genes (Cord Neto et al., 1995; Schmidt et al., 2011; Li et al., 2015). The maize endosperm-specific Dof (DNA binding one zinc finger) transcription factor (TF), prolamin box binding factor1 (PBF1), specifically recognizes the prolamin box to regulate 22-kD α-zein and 27-kD γ-zein genes (Vicente-Carbajosa et al., 1997; Wu and Messing, 2012). Likewise, rice O2-like protein, bZIP58 (also called RISBZ1) and the PBF subfamily member RPBF also play a role in the regulation of storage protein synthesis. Individual knockdown mutants of *bZIP58* and *RPBF* show little change in most storage proteins, but a double knockdown mutant has a pronounced decrease of most storage protein, as bZIP58 and RPBF are able to directly activate the expression of *GluA1*, *GluA2*, *GluA3*, *GluB1*, *GluD1*, *10 kD Prolamin*, *13 kD prolamin*, and *16 kD prolamin* (Yamamoto et al., 2006; Kawakatsu et al., 2009). In addition, maize O2 hetero-dimerizing protein1 (OHP1), OHP2, ZmbZIP22, and ZmMADS47 also can regulate zein gene transcription directly (Zhang et al., 2015; Qiao et al., 2016; Li et al., 2018a).

There are several TFs showing a regulation role in both protein and starch metabolism. Apart from the function in zein regulation, O2 and PBF1 also play a role in starch synthesis by directly binding to the promoters of *PPDK1*, *PPDK2*, and *SSIII* and by indirect regulation of *SSIIa* and *SBEI* (Zhang et al., 2016). Likewise, OsbZIP58 not only regulates storage protein accumulation, it can also bind directly to the promoters of the starch synthesis-related genes *OsAGPL3*, *Wx*, *OsSSIIa*, *SBE1*, *OsBEIIb*, and *ISA2* to regulate their expression (Wang et al., 2013; Kim et al., 2017). OPAQUE11 (O11), a basic helix-loop-helix-type TF, directly modulates O2 and PBF1, which gives it a modulated function in both starch and storage protein accumulation (Feng et al., 2018). Recently, Zhang et al. (2019b) reported that deficiency of *ZmNAC128* and *ZmNAC130* decreases starch and protein accumulation, as ZmNAC128 and ZmNAC130 directly regulate *16-kD γ-zein* and *AGPS2* (*Bt2*) expression by binding to their promoters.

In general, starch and storage protein syntheses have been comprehensively investigated, but the plant regulators responsible for the syntheses remain largely unknown. NAM, ATAF1/2, and CUC2 (NAC) TFs are one of the largest plant-specific TF families (Souer et al., 1996; Aida et al., 1997; Zhao et al., 2016a). The most notable feature of the NAC TF family is that they contain a conserved NAC domain responsible for the binding properties in the N terminus. The C terminus of NAC TFs normally confers a diversified transcriptional regulatory region (TRR) that contributes to its activation or repression properties (Ooka et al., 2003; Olsen et al., 2005). NAC TFs have been reported to participate in various processes, such as biotic and abiotic stress responses, formation of a secondary cell wall, senescence, meristem regulation, and so on (Kubo et al., 2005; Fang et al., 2008; Yamaguchi et al., 2008; Balazadeh et al., 2011; Wu et al., 2012; Mao et al., 2017; Li et al., 2019; Sun et al., 2019, Sakuraba et al., 2020). However, their functions in the endosperm have not been fully elucidated.

A search of transcriptome data, a rice expression profile database (http://ricexpro.dna.affrc.go.jp/), and published papers (Fang et al., 2008; Nie et al., 2013; Mathew et al., 2016) yielded eight endosperm-specific NAC TFs: OsNAC20 (LOC_Os01g01470/Os01g0104500), OsNAC23 (LOC_Os02g12310/ Os02g0214500), OsNAC24 (LOC_Os05g34310/Os05g0415400), OsNAC25 (LOC_Os11g31330/Os11g0512000), OsNAC26 (LOC_Os01g29840/Os01g0393100), OsNAC127 (LOC_Os11g31340/Os11g0512100), OsNAC128 (LOC_Os11g31360/ Os11g0512200), and OsNAC129 (LOC_Os11g31380/Os11g0512600). Herein, the most highly expressed *OsNAC26* (previously *ONAC026*) and its homologous gene, *OsNAC20* (previously *ONAC020*), were selected for further analysis to detect whether they

have a function in rice endosperm. We employed a reverse genetic approach to unveil the functions of OsNAC20 and OsNAC26 in synthesizing starch and storage protein in rice endosperm. Clustered regularly interspaced short palindromic repeats (CRISPR)/CRISPR-associated protein 9 (Cas9)-generated *osnac20* and *osnac26* single mutants showed no alterations in their grain phenotype, but their double mutant, *osnac20/26*, displayed a floury grain caused by decreased starch and storage protein content. A series of assays were utilized to determine the target genes of OsNAC20 and OsNAC26. These results could enrich our knowledge of the regulatory network of starch and storage protein synthesis and accumulation.

RESULTS

OsNAC20 and *OsNAC26* Are Specifically Expressed in Grain

OsNAC20 and *OsNAC26* share 89% sequence similarity in their coding sequence (CDS) and 85% sequence similarity in their amino acid sequence (Supplemental Fig. S1). Reverse transcription quantitative PCR (RT-qPCR) analysis showed that *OsNAC20* and *OsNAC26* were not detectable in a range of organs, including the root, stem, leaf, panicle, leaf sheath, embryo, and pericarp, but were expressed only in developing endosperm, with a peak at 13 d after flowering (DAF; Fig. 1, A and B; Supplemental Fig. S2A). The protein level was further analyzed by immunoblot. Anti-OsNAC20 and anti-OsNAC26 were produced against the synthetic peptide CRIFHKSSGIKKPVPVAPHQ and the expressed protein (160–333 amino acids), respectively (Supplemental Fig. S2B). The protein sizes for OsNAC20 and OsNAC26 are 35.74 and 37.39 kD, respectively. As shown in Figure 1, C and D, only one band was observed at ~36 kD for anti-OsNAC20, but two bands were observed, at ~36 kD and 38 kD, for anti-OsNAC26, which indicated that the anti-OsNAC20 is specific but anti-OsNAC26 can detect both OsNAC20 and OsNAC26. Interestingly, OsNAC20 and OsNAC26 both were detected not only in endosperm but also in the embryo at the protein level, although no mRNA in the embryo was detected by RT-qPCR assays (Fig. 1, A–D). In endosperm, OsNAC26 was expressed after 4 DAF, while OsNAC20 showed an obvious protein level at 10 DAF (Fig. 1D). Immunofluorescence assays with anti-OsNAC20 and anti-OsNAC26 showed that the fluorescence signals were situated in the nuclei of starchy endosperm and the aleurone layer (Fig. 1, E–G). The signals were also broadly distributed in the whole embryo nuclei (Fig. 1, H–J). In addition, subcellular localization of 35S:OsNAC20-GFP and 35S:OsNAC26-GFP expressed in *Nicotiana benthamiana* leaves was concentrated in the nuclei (Supplemental Fig. S3), which indicated that both OsNAC20 and OsNAC26 function in the nucleus. In conclusion, *OsNAC20* and *OsNAC26* are grain-specific instead of endosperm-specific genes, as both were located in nuclei of the aleurone layer, starchy endosperm, and embryo.

OsNAC20 and OsNAC26 Can Interact with Each Other

To determine whether OsNAC20 and OsNAC26 can form homo- or heterodimers, we performed bimolecular fluorescence complementation assays. Both OsNAC20 and OsNAC26 interacted with themselves (Supplemental Fig. S4A). More importantly, OsNAC20 and OsNAC26 could interact with each other in the nuclei (Supplemental Fig. S4A), which is consistent with the result for onion (*Allium cepa*) epidermal cells (Mathew et al., 2016). A His pull-down assay confirmed their heterodimerization (Supplemental Fig. S4B). Therefore, OsNAC20 can physically interact with OsNAC26 in plant cell nuclei.

Phylogenetic Analysis of OsNAC20 and OsNAC26

The most similar proteins to OsNAC20 and OsNAC26 are from wild rice species (*Oryza* spp.; Supplemental Fig. S5). Their whole protein sequences share 43% to 72% similarity with OsNAC20 and OsNAC26. The sequence similarity of other homologous proteins is limited to the NAC domain, which shows ~70% similarity with OsNAC20 and OsNAC26. Phylogenetic analysis indicated that these homologous proteins with known functions are ZmNAC128 and ZmNAC130 in maize, and AtNAC87 in Arabidopsis. ZmNAC128 and ZmNAC130 have been reported to take part in the regulation of storage product accumulation (Zhang et al., 2019b). Expression of *AtNAC87* is changed in response to *Cabbage leaf curl virus* in Arabidopsis (Ascencio-Ibáñez et al., 2008). These results indicated that OsNAC20 and OsNAC26 might play a role in storage product synthesis and stress response.

Simultaneous Deficiency of *OsNAC20* and *OsNAC26* Results in Floury Grains

To investigate whether deficiency of *OsNAC20* and/or *OsNAC26* affects grain development, we generated knockout mutants through the CRISPR/Cas9 technique. Each target locus was scanned for possible off-target matches through mapping of the whole genome (http://cbi.hzau.edu.cn/cgi-bin/CRISPR; Supplemental Table S1) to ensure the specificity of these target sequences.

Two targets in the CDS regions were mutated to derive the single mutant for each gene, and the resulting mutants were designated as *osnac20-1*, *osnac20-2*, *osnac26-1*, and *osnac26-2* (Supplemental Fig. S1A). For *osnac20-1* and *osnac26-1*, unfortunately, we didn't genotype the corresponding single mutants, as the target sequences for these two mutants were highly similar and both genes were mutated in the two single mutants. The target for *osnac20-2* is specific and no possible off-target sequence was detected (Supplemental Fig. S1A;

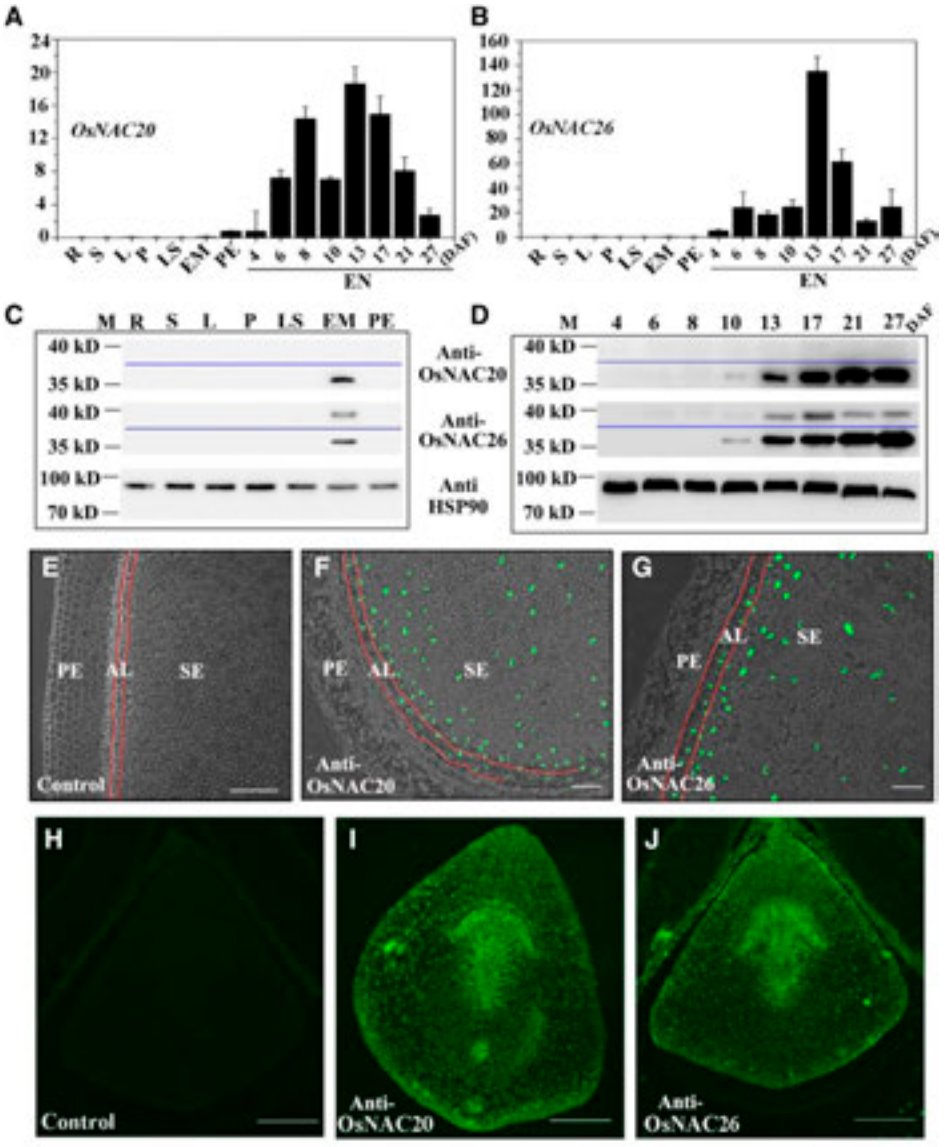

Figure 1. Expression analysis of *OsNAC20* and *OsNAC26* in rice. A and B, RT-qPCR analysis of *OsNAC20* and *OsNAC26* expression in different organs and in developing endosperms (EN) of cv ZH11. Actin was used as an internal control. The *y* axis represents the expression level relative to that of the control. Samples of root (R), stem (S), leaf (L), and leaf sheath (LS) were derived from plants at the four-leaf stage. Panicles (P) were harvested at 3 d before heading. Both pericarp (PE) and embryo (EM) tissues were collected from developing caryopses at 8 DAF. Three biological experiments (three technical replicates for each biological experiment) were conducted in A and B. Values are means ± SD. C and D, Immunoblot analysis of OsNAC20 and OsNAC26 expression profiles in different organs and developing endosperms. HSP90 antibody was used as a sample loading control. Total protein samples were extracted from pooled tissues. M, Protein marker. E to J, Immunofluorescence assays of OsNAC20 and OsNAC26 in endosperm (E–G) and embryo (H–J) at 8 DAF. Both endosperm and embryo were transversely sectioned. Samples without anti-OsNAC20 and anti-OsNAC26 were used as control (E and H). AL, Aleurone layer; SE, starchy endosperm. Scale bars = 150 μm.

Supplemental Table S1). Although the target site for *osnac26-2* was also similar to the counterpart of *OsNAC20*, *OsNAC20* was not mutated in the *osnac26-2* mutant (Supplemental Figs. S1A and S6A; Supplemental Table S1). Therefore, the *osnac20-2* and *osnac26-2* mutants were used for further analysis. As shown in Supplemental Fig. S7, the single mutation of *OsNAC20* and *OsNAC26* had no effect on grain development.

The sites targeted for *osnac20-1* and *osnac26-1* were mutated to effectively derive the double mutant (Fig. 2, A and B; Supplemental Fig. S1A). Two homozygous independent double mutants were named *osnac20/26-1* and *osnac20/26-2* (Fig. 2, A and B). The possible off-target risk in *OMTN1* (*LOC_Os02g36880*) in the double mutant was excluded (Supplemental Fig. S6B; Supplemental Table S1). Immunoblot analysis verified the loss of function of OsNAC20 and OsNAC26 in the two mutants (Fig. 2C). Phenotypic characterization showed no detectable change in such traits as plant height, panicle number, and flowering date was observed in the *osnac20/26-1* and *osnac20/26-2* mutants compared to cv Zhonghua11 (ZH11; Supplemental Fig. S8A), but the mutant grains showed a floury phenotype (Fig. 2D). The grain width, thickness, and 1,000-grain weight were significantly reduced (Fig. 2, E–H). Follow-up phenotyping of the two mutants revealed a consistent grain phenotype (Supplemental Fig. S8, B–F), which further indicated that this phenotype was caused by the deficiency of *OsNAC20* and *OsNAC26*. The *osnac20/26-1* line was used for further study in the following experiments.

Simultaneous Deficiency of *OsNAC20* and *OsNAC26* Results in a Significant Decrease in Starch Accumulation

Shape observation of developing caryopsis showed no obvious differences between cv ZH11 and *osnac20/*

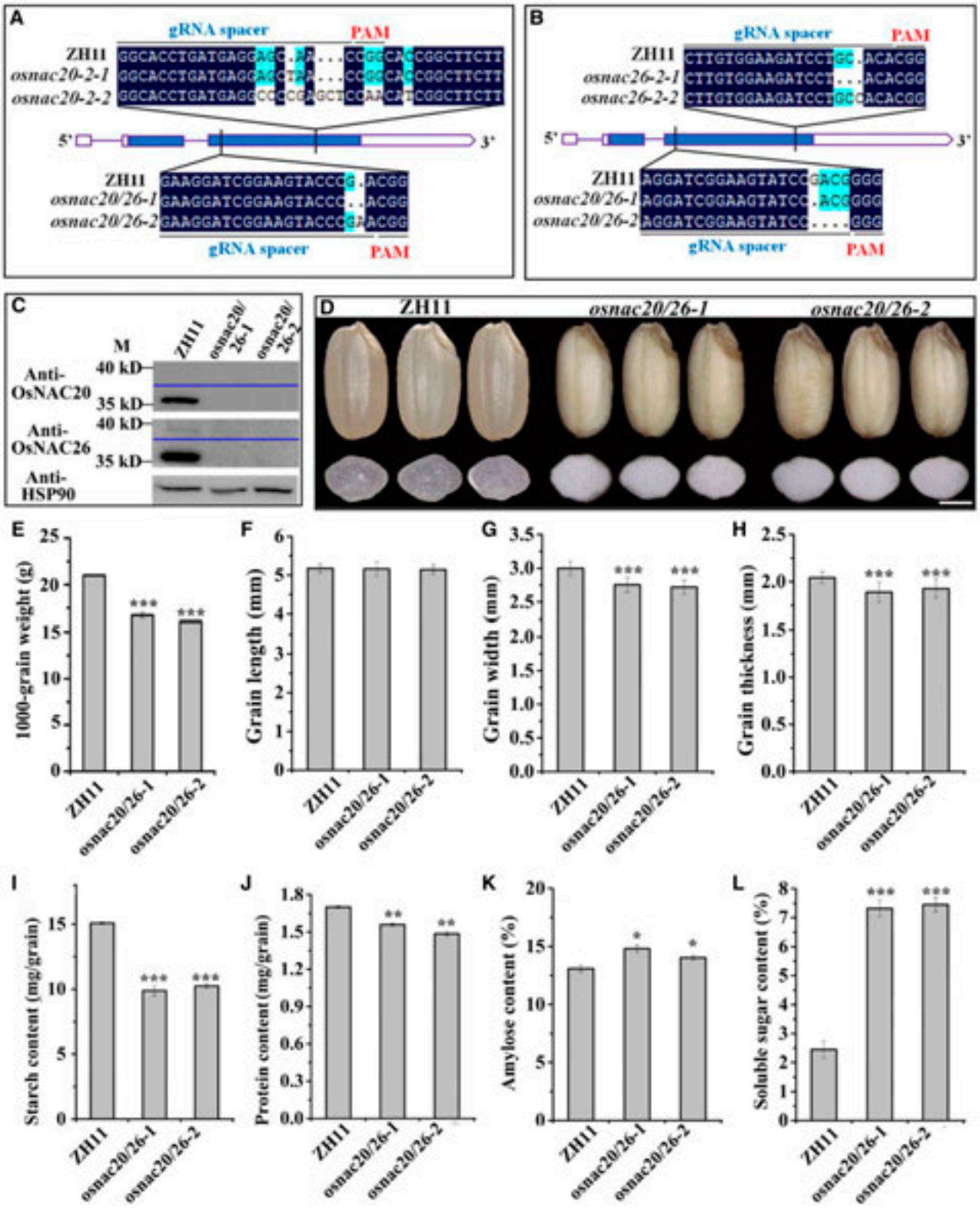

Figure 2. Mutation sequence and seed phenotypic analysis of the *osnac20/26* mutant. A and B, Mutation of the CDS in *OsNAC20* (A) and/or *OsNAC26* (B) mutants. Two homozygous independent transgenic plants were derived for each mutation. All of these mutations resulted in loss of function of OsNAC20 and OsNAC26 due to a frame shift. Solid boxes represent the exons, solid lines the introns, and open boxes the untranslated region. C, Immunoblot analysis of anti-OsNAC20 and anti-OsNAC26 in the *osnac20/26* double mutant. Anti-HSP90 antibody was used as the internal control. Total proteins were extracted from pooled

26-1 caryopses before 4 DAF, but the *osnac20/26-1* caryopsis became smaller after 4 DAF, and this difference was continuously detected with caryopsis development and was ascribed to defective dry matter accumulation (Fig. 3, A and B). In rice grains, most of the dry matter is starch. Two lines of evidence indicated that the significantly decreased dry matter/grain weight in the *osnac20/26-1* mutant was mainly due to the significantly reduced starch content (Fig. 2I). First, the grain-filling rate was reduced in the *osnac20/26-1* mutant after 4 DAF (Fig. 3B). Second, the starch granules in the *osnac20/26-1* mutant were always packed less tightly than the corresponding region of cv ZH11 during the development stage (Fig. 3C).

Interestingly, the morphology of starch granules did not show a significant difference between cv ZH11 and the *osnac20/26-1* mutant, both of which displayed a polygonal shape in the central, dorsal, ventral, and lateral regions of the kernel. It was only that the size of starch granules in the mutant was less homogeneous than that of the control (Supplemental Fig. S9, A and B). The starch also showed a similar M_r distribution, except that the amylose content of the mutant was slightly higher than that of the control (Supplemental Fig. S9C; Supplemental Table S2), which was consistent with the results obtained from the iodine colorimetric method (Fig. 2K). In addition, starches from cv ZH11 and *osnac20/26* had an A-type crystalline structure and similar gelatinization properties (Supplemental Fig. S9, D and E). Overall, the deficiency of *OsNAC20* and *OsNAC26* significantly changed starch accumulation but did not have a remarkable influence on starch morphology, molecular structure, and physicochemical properties.

Simultaneous Deficiency of *OsNAC20* and *OsNAC26* Results in a Pronounced Decrease in Storage Protein Content and a Defective Protein Body

Apart from starch, storage protein is also an important component of dry matter in rice grains. The storage protein amount showed a pronounced decrease in the *osnac20/26* mutant (Fig. 2J). The storage proteins accumulate in the protein body (PB), and therefore, the PB was further investigated using semithin sections stained with acid fuchsin and Coomassie brilliant blue, two dyes that are specific for protein staining (Fig. 4, A and B; Supplemental Fig. S10). The PBs were mainly distributed in the subaleurone region in cv ZH11 and *osnac20/26-1* plants, but those in the double mutant were less densely packed than those in the control (Fig. 4, A and B; Supplemental Fig. S10). Furthermore, the number and area of PBs were investigated by transmission electron microscopy (TEM). PBI, which derives from the endoplasmic reticulum (ER) and consists of prolamin, showed spherical morphology and was surrounded by rough ER attached with ribosomes (Fig. 4C). Glutelin- and globulin-containing PBII accumulated in protein storage vacuoles (PSVs) and displayed an irregular shape (Fig. 4C). Although PBI morphology was similar in the *osnac20/26-1* mutant, the density and area were decreased by ~40% and 30%, respectively (Fig. 4, E and F). With regard to PBII, its filling was significantly affected. As shown in Figure 4D, PSVs were not completely occupied by storage proteins, and in some cases were empty, resulting in an extremely small PBII area in the *osnac20/26-1* mutant compared to cv ZH11 (Fig. 4F). The above results indicated that storage protein synthesis is severely affected in this double mutant.

Identification of Genes Regulated by OsNAC20 and OsNAC26

RNA-sequencing (RNA-seq) analysis was conducted to investigate the molecular mechanism of phenotypic defects in the *osnac20/26* mutant (Supplemental Fig. S11). A total of 2,564 differentially expressed genes (DEGs) were characterized, including 1,631 downregulated genes and 933 upregulated genes (Supplemental Table S3). The Gene Ontology (GO) enrichment termed "response to stress" suggested again a potential function of OsNAC20 and OsNAC26 in stress, which is consistent with the result of phylogenetic analysis (Fig. 5A; Supplemental Fig. S5). Most importantly, the "nutrient reservoir" terms, mainly including glutelin, prolamin, and globulin synthesis-related genes, broadly changed expression profile in the *osnac20/26-1* mutant; in which 11 DGEs were downregulated, and the reduction levels ranged from 68% to 93% (Table 1). Furthermore, we detected that several starch synthesis-related genes, including *AGPS2b*, *AGPL2*, *SSI*, *SBEI*, *Pul*, and *DPEI*, were significantly downregulated (Table 1). Among them, the transcription levels of *AGPS2b* and *Pul* were most markedly decreased, by 91.3% and 93.6%, respectively. RT-qPCR confirmed the decreased expression levels of these DGEs (Supplemental Fig. S12A).

Figure 2. (*Continued.*)
endosperm samples at 13 DAF. M, Protein marker. D, Grain phenotypic features of cv ZH11, *osnac20/26-1*, and *osnac20/26-2*. Images shown were digitally extracted and scaled for comparison. Scale bar = 1.5 mm. E to H, Measurement of 1,000-grain weight (E), grain length (F), grain width (G), and grain thickness (H) of the wild type and the *osnac20/26* mutant ($n = 3$ [E] and 50 [F–H]). I to L, Starch content (I), storage protein content (J), amylose content (K), and soluble sugar content (L) in mature grains of cv ZH11 and the *osnac20/26* mutant. Data in E to L were measured from mature grains. Values are means ± SD from two (J and K) and three (I and L) biological replicates. The asterisk indicates a statistically significant difference between cv ZH11 and the *osnac20/26* mutants, as calculated by Student's *t* test (*$P < 0.05$, **$P < 0.01$, and ***$P < 0.001$).

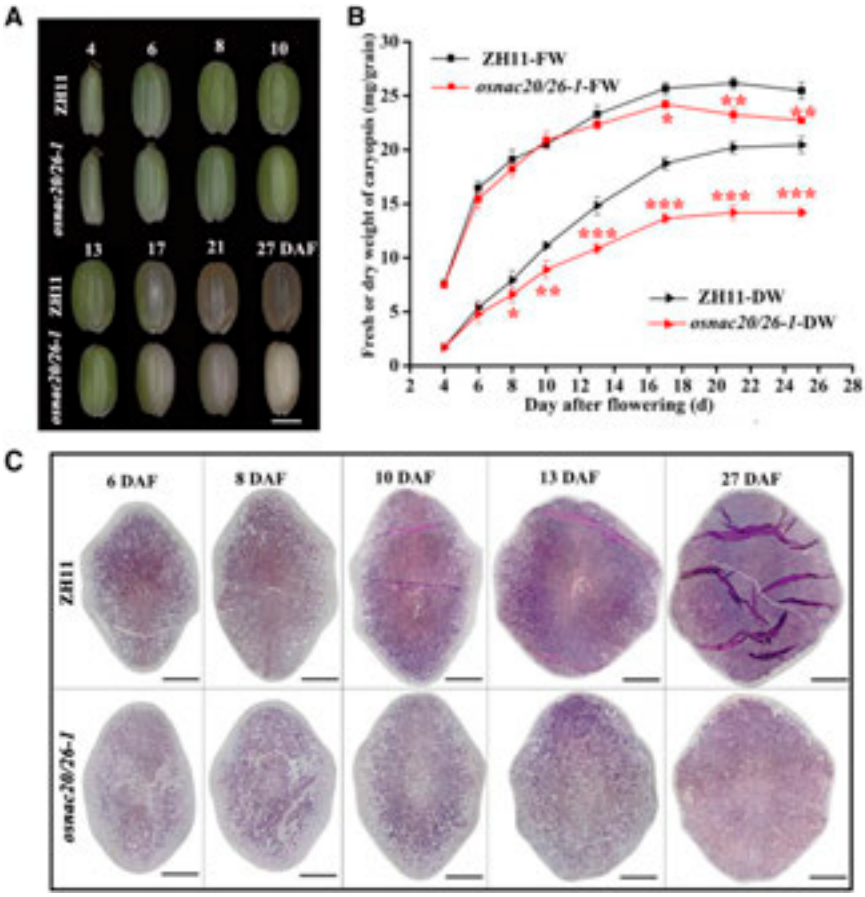

Figure 3. Phenotype, weight, and starch accumulation in developing caryopsis of the *osnac20/26-1* mutant. A, Phenotype of the developing caryopsis. Scale bar = 2 mm. B, Fresh weight (FW) and dry weight (DW) of developing caryopsis. Thirty caryopses from the same part of three plants (10 for each plant) were considered as one replicate, and the weight of one caryopsis was calculated. Three replicates were conducted. Values are means ± SD. The asterisk indicates a statistically significant difference between cv ZH11 and the *osnac20/26-1* mutant, as calculated by Student's *t* test (*$P < 0.05$, **$P < 0.01$, and ***$P < 0.001$). C, Microphotographs of iodine-stained transverse sections of developing caryopses at the midregion. Scale bars = 0.5 mm. Images shown in A and C were digitally extracted and scaled for comparison.

Next, SDS-PAGE, immunoblot, and/or enzyme activity assays were performed in rice endosperm to examine whether the change in RNA expression of these DEGs affected the protein amount and/or enzyme activity. Similar to the reduced protein abundance, SSI and DPE1 activities were decreased by ~34% and 80%, respectively. Pul activity was decreased ~70% (Fig. 5, B–G). However, the activity levels of AGPase and SBE in the *osnac20/26-1* mutant were not significantly different from those in cv ZH11, although *AGPS2b*, *AGPL2*, and *SBEI* were remarkably downregulated (Fig. 5, E and G; Table 1). In addition, the protein abundance of some other starch synthesis-related enzymes was similar between cv ZH11 and the double mutant, as was the RNA level (Supplemental Fig. S12B; Supplemental Table S3).

For storage proteins, decreased accumulation of glutelin acidic and basic subunits was detected in the mutant compared to cv ZH11 (Fig. 5H). When further separating glutelin acidic subunits, it was detected that the GluA2 band was not significantly different between cv ZH11 and *osnac20/26-1*, and the GluA1 abundance was slightly lower in the mutant than in cv ZH11, while GluB4 was severely decreased in the *osnac20/26-1* mutant compared to cv ZH11 (Fig. 5H). Immunoblot analysis indicated that total GluA and GluB acidic subunits were decreased by ~17% and 32%, respectively, in the *osnac20/26-1* mutant compared to cv ZH11 due to the respective reductions in GluA1 and GluB4 (Fig. 5I). Most notably, α-globulin and 16 kD prolamin were almost completely absent from the *osnac20/26-1* mutant (Fig. 5, H and I). These data indicated that decreased starch and storage protein synthesis are mainly attributed to the reduced expression of starch and storage protein synthesis-related genes, and they further suggested possible roles of OsNAC20 and OsNAC26 in the regulation of starch and storage protein synthesis in rice endosperm.

OsNAC20 and OsNAC26 Directly Target Endosperm Starch and Storage Protein Synthesis-Related Genes

According to RNA-seq, RT-qPCR, SDS-PAGE, immunoblot, and enzyme activity assay results, starch and storage protein synthesis-related genes, including *AGPS2b*, *AGPL2*, *SSI*, *SBEI*, *Pul*, *DPE1*, *α-glolulin*, *16 kD prolamin*, *GluB4*, and *GluA1*, were further investigated through a dual-luciferase (dual-luc) reporter assay to detect whether they can be directly transactivated by OsNAC20 and/or OsNAC26 (Figs. 5 and 6; Table 1). As shown in Figure 6, B to K, both OsNAC20 alone and OsNAC26 alone transactivated these genes well except in the case of DPE1; however, their activation level varied among different promoters. For example, OsNAC20 showed a 323-fold

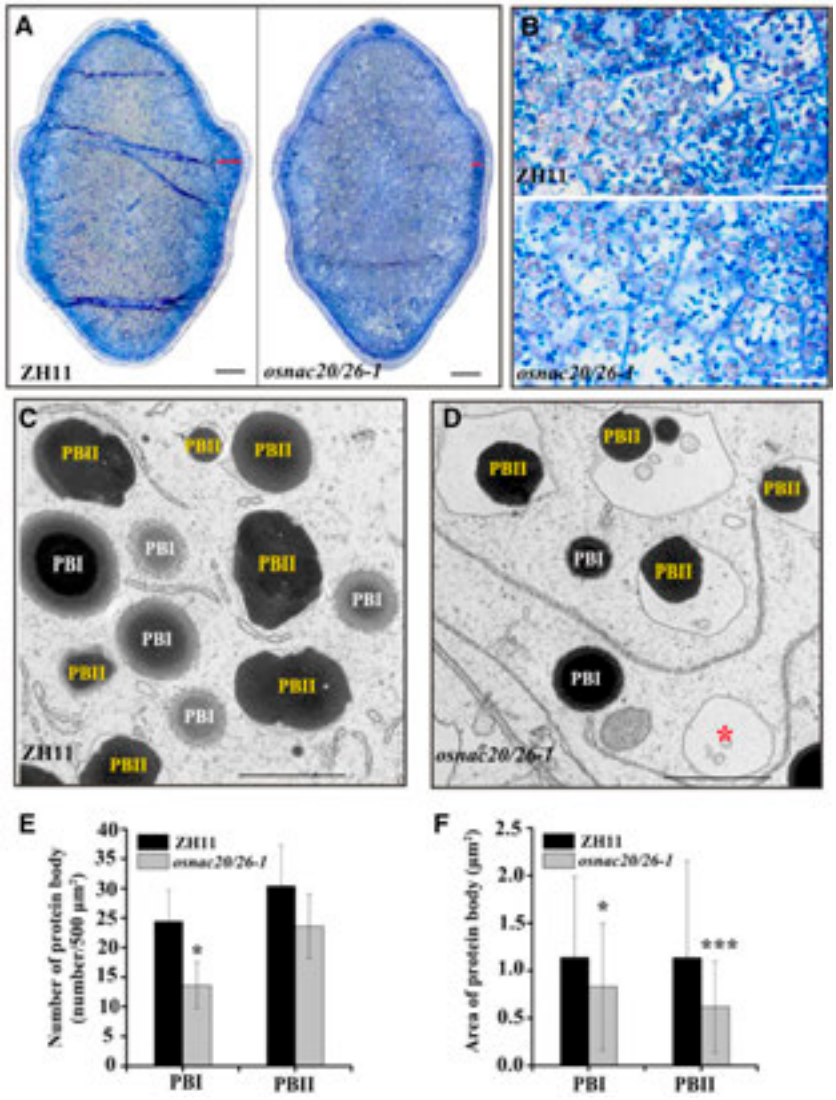

Figure 4. Storage protein analysis in endosperm of the *osnac20/26-1* mutant. A, Microphotographs of Coomassie brilliant blue-stained transverse sections of midregion caryopses from cv ZH11 (left) and *osnac20/26* (right) at 10 DAF. Scale bar = 0.3 mm. B, Images are magnifications of the regions marked by a red line at the far right in the full-scale images of A (left and right, respectively). Scale bars = 10 μm. C and D, TEM photographs of PBI and PBII in endosperm of cv ZH11 (C) and *osnac20/26* (D) at 10 DAF. The red asterisk in D indicates the empty PSV in the *osnac20/26-1* mutant. Scale bars = 2 μm. Images shown in A to D were digitally extracted and scaled for comparison. E and F, Number and area of the PB in the same endosperm region of cv ZH11 and *osnac20/26* at 10 DAF. Numbers of PBs were counted in the TEM photographs with the same magnification and area (500 μm^2), and their means and SDs were calculated from five TEM photographs. The areas of PBI and PBII were individually measured using Photoshop Software, and their means and SDs were calculated from all PBs in the above-mentioned five TEM photographs. The asterisk indicates a statistically significant difference between cv ZH11 and the *osnac20/26-1* mutant, as calculated by Student's *t* test (*$P < 0.05$ and ***$P < 0.001$).

luciferase increase in activating the *AGPS2b* promoter, but OsNAC26 only produced a 117-fold increase; with regard to the *16 kD prolamin* promoter, the two proteins showed a similar activation level, but coexpression did not enhance the *LUC* expression level compared to that of OsNAC20 or OsNAC26 alone. This result indicated that although OsNAC20 and OsNAC26 can interact with each other, they independently regulated the expression of starch and storage protein synthesis-related genes.

To further confirm the binding of OsNAC20 and OsNAC26 to these gene promoters, an electrophoretic mobility shift assay (EMSA) was conducted. As shown in Supplemental Table S4, the promoters of *AGPL2*, *SSI*, *SBEI*, *Pul*, *GluB4/5*, and *16 kD prolamin* contain the ACGCAA motif, an element that has been reported to interact with maize NAC TFs to take part in storage product accumulation (Zhang et al., 2019b). Among these, *SBEI* and *16 kD prolamin* promoters were further investigated to demonstrate their interaction with OsNAC20 and OsNAC26. The result showed that OsNAC20 and OsNAC26 were able to bind to the ACGCAA motif (Fig. 7, A and B; Supplemental Table S5). In the case of *AGPS2b*, there is no ACGCAA motif in its promoter. Therefore, the truncated *AGPS2b* promoters were produced to detect the cis-element targeted by OsNAC20 and OsNAC26. As shown in Figure 8, A and B, compared to the F+R, F1+R and F2+R fragments, which displayed strong transactivation activity, F3+R showed significantly decreased activity, F4+R demonstrated relatively weak activity, and F5+R had no activity. This result placed the cis-element at the −340, −286, and −177 sites in the *AGPS2b* promoter, especially the −340 site, which is mainly responsible for the binding activity. EMSA results showed that DNA sequences that contain the −340 and −286 sites were specifically bound by OsNAC20 and OsNAC26, respectively, but those containing the −177 fragment were not, which might be because some other NAC

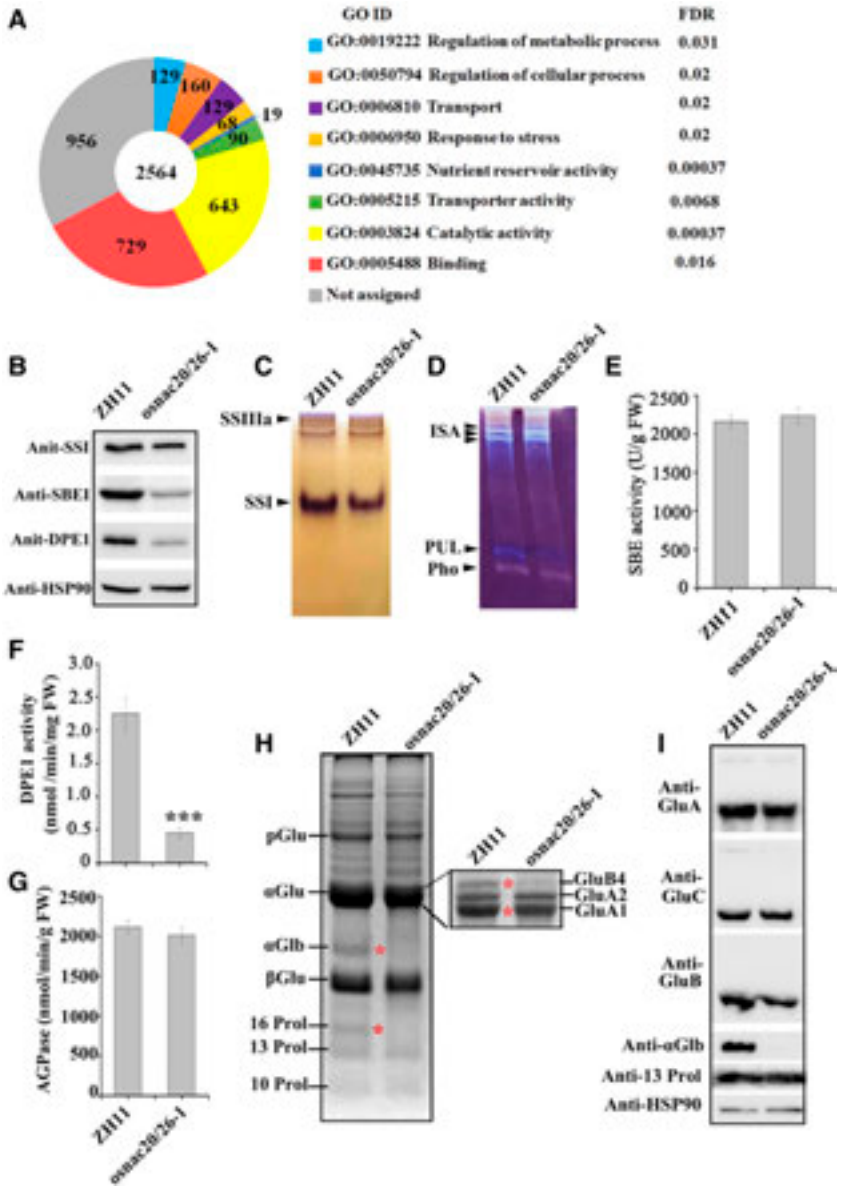

Figure 5. Genome-wide analyses of the OsNAC20- and OsNAC26-regulated network. A, GO classification of DEGs from the *osnac20/26-1* RNA-seq analysis. The changes in gene expression level were calculated from three biological replicates (fold change >2.5 and $Q < 0.001$). Enrichment analysis of functional categories was performed at the agriGO Web site (http://bioinfo.cau.edu.cn/agriGO/analysis.php). The RNA sample for each replicate was extracted from independent pools of endosperm at 10 DAF. The numbers of genes classified within each GO term, as well as their Q values, are shown. Only GO terms with at least 10 annotated genes were kept. B, Immunoblot analysis of starch synthesis-related proteins in rice endosperm at 10 DAF. C and D, Native-PAGE/activity staining analysis of SS (C) and DBE (D). E to G, Activity of SBEI (E), DPE1 (F), and AGPase (G). Total protein samples were extracted from pooled endosperm at 10 DAF. Values are means ± SD from three biological replicates. The asterisk indicates a statistically significant difference between cv ZH11 and the *osnac20/26-1* mutant as calculated by Student's t test (***$P < 0.001$). H, SDS-PAGE analysis of storage proteins in mature endosperm from cv ZH11 and the *osnac20/26* mutant. Red asterisks indicate the bands in the *osnac20/26* mutant that are different from those of cv ZH11. The inset shows the αGlu further separated with a higher polyacrylamide concentration gradient gel and lower electric tension. I, Immunoblot analysis of storage protein synthesis-related proteins in mature endosperm. HSP90 was used as a loading control. pGlu, Glutelin precursors; αGlu, glutelin acidic subunits; βGlu, glutelin basic subunits; αGlb, α-globulin; 10 Prol, 13 Prol, and 16 Prol represent 10-kD, 13-kD, and 16-kD prolamin, respectively.

binding sites exist in it (Figs. 7A and 8C; Supplemental Table S5). Although there is also no ACGCAA element in the *GluA1* and *α-glolulin* promoters, they contain the core binding sites of the −340 binding site (Supplemental Table S4).

Previous studies have reported that subdomains C and D in the NAC domain may interact with cis-acting elements (Wang and Culver, 2012). We generated two truncated versions of OsNAC20 and OsNAC26, $OsNAC20^{NAC}$, $OsNAC26^{NAC}$, and $OsNAC20/26^{CD}$, and tested the binding of these three proteins to the target sequence to investigate whether the NAC domain or C and D subdomains are required for DNA binding. Results showed that the NAC domain, but not the C and D subdomains, was able to bind to the cis-elements (Fig. 7C), which might be due to the fact that except for the C and D subdomains, other subdomains are also required for assistance in binding to DNA sequences.

DISCUSSION

Expression Patterns of *OsNAC20* and *OsNAC26* in Seeds

The thinner caryopsis phenotype and decreased dry weight after 4 DAF in the *osnac20/26* mutant indicated that OsNAC20 and OsNAC26 function after 4 DAF in the caryopsis. Starch and storage protein contents significantly increased between 4 and 10 DAF, and few of them are synthesized at the late developing stage (after 17 DAF; Fig. 3B; Yamagata et al., 1982). However, only faint bands of OsNAC20 and OsNAC26 were detected between 4 and 10 DAF, whereas higher content of these

Table 1. *Decreased expression of starch- and storage protein synthesis-related genes*

Gene Identifier (RAP_Locus)	Gene Name	Fold Change	False Discovery Rate
Os08g0345800	*AGPS2b*	0.087	8.86E−41
Os01g0633100	*AGPL2*	0.279	3.17E−48
Os06g0160700	*SSI*	0.358	3.66E−32
Os06g0726400	*SBEI*	0.201	8.01E−09
Os04g0164900	*Pul*	0.064	8.34E−14
Os07g0627000	*DPE1*	0.399	1.56E−17
Os01g0762500	*GluA1*	0.268	3.79E−07
Os10g0400200	*GluA2*	0.320	7.86E−07
Os02g0249800	*GluB-1a*	0.222	2.63E−06
Os02g0249900	*GluB-1b*	0.165	5.57E−14
Os02g0249600	*GluB2*	0.205	0.00012
Os02g0268300	*GluB4*	0.136	0.00064
Os02g0268100	*GluB5*	0.105	0.00091
Os02g0453600	*GluC*	0.157	1.80E−05
Os05g0499100	*α-globulin*	0.114	3.66E−12
Os07g0206400	13 kD prolamin	0.072	9.42E−06
Os06g0507200	16 kD prolamin	0.077	4.92E−38

proteins was observed at the late stage (Fig. 1D). It is inferred that OsNAC20 and OsNAC26 might have a function in late seed development. Interestingly, we observed a preharvest sprouting phenotype (Supplemental Fig. S13), which is related to ABA-controlled seed dormancy. After 17 DAF, the seed prepares to enter into the dormancy stage. Combined with the down-regulated *OsRCAR1* (Os06g0527800; ABA receptor) expression in the double mutant (Supplemental Table S3), we reasonably speculated that OsNAC20 and OsNAC26 might have a function in controlling seed dormancy.

In previous studies, *OsNAC20* and *OsNAC26* are reported as endosperm-specific genes, as embryo tissue was not included in the investigated organs (Fang et al., 2008; Nie et al., 2013). In this study, *OsNAC20* and *OsNAC26* transcripts were not detected in the embryo at 8 DAF, but their proteins were detected by immunoblot and immunostaining at this stage (Fig. 1, A–D and H–J), which might be due to the fact that mRNA is transcribed first, followed by protein translation.

OsNAC20 and OsNAC26 Regulate Starch Synthesis

In the *osnac20/26-1* mutant, the starch content was reduced by ~30% (Figs. 2I and 3B), which was attributed to the reduced expression and activity of SSI, Pul, and DPEI instead of the unchanged AGPase and SBE activity, although OsNAC20 and OsNAC26 can bind to the promoters of *AGPS2b*, *AGPL2*, and *SBEI* to regulate their expression (Figs. 5–8; Table 1).

Several studies have reported that the cytosolic isoforms, including AGPS2b and AGPL2 in rice and AGPS1a (Bt2) and AGPL1 (Sh2) in maize, are mainly responsible for the AGPase activity in endosperm. Any mutation of these four genes can produce a significant reduction of AGPase activity, resulting in a shrunken seed phenotype due to the marked decrease of starch synthesis (Yano et al., 1984; Giroux and Hannah, 1994; Tuncel et al., 2014). One interesting result worth noting in the *osnac20/26-1* mutant is that although the expression levels of *AGPS2b* and *AGPL2* were markedly decreased, the AGPase activity in this double mutant paralleled that of cv ZH11 (Fig. 5G; Table 1). Therefore, the decreased starch content in the *osnac20/26-1* mutant is unrelated to the reduced expression of *AGPS2b* and *AGPL2*. A similar case is detected in the mutant of *ZmbZIP22*, a gene that encodes a bZIP-type TF and regulates the *27-kD γ-Zein* gene in maize (Li et al., 2018a). In the *zmbzip22* mutant, the expression of *AGPS1a* and *AGPL1* are also significantly reduced. Although AGPase activity was not examined in the study of Li et al. (2018a), we speculate that it is unchanged, as the total starch level is essentially unchanged in the *zmbzip22* mutant. Furthermore, we investigated the gene expression of other plastid-localized AGPase subunits in *osnac20/26-1* endosperm, and the results showed that the expression levels of *AGPS1* (*Os09g0298200*) and *AGPL3* (*Os03g0735000*) were not significantly different between cv ZH11 and the *osnac20/26-1* mutant, and that of *AGPL1* (*Os05g0580000*) was ~58% reduced in the mutant (Supplemental Table S3). This indicated that AGPase complementation did not happen in this double mutant. A recent study has reported that AGPase is phosphorylated in wheat seeds, which indicated that AGPase can undergo posttranslational modification (Ferrero et al., 2020). Therefore, we inferred that the lack of change in AGPase activity in the *osnac20/26* mutant might have been due to posttranslational modification of the residual transcripts of *AGPS2b* and *AGPL2*, which could maintain full AGPase activity.

OsNAC20 and OsNAC26 can bind to the *SBEI* promoter to regulate its expression, but the total SBE activity was not decreased in the double mutant. Two possibilities exist: either the SBEI activity was not changed, although its RNA and protein levels were decreased, or the reduced

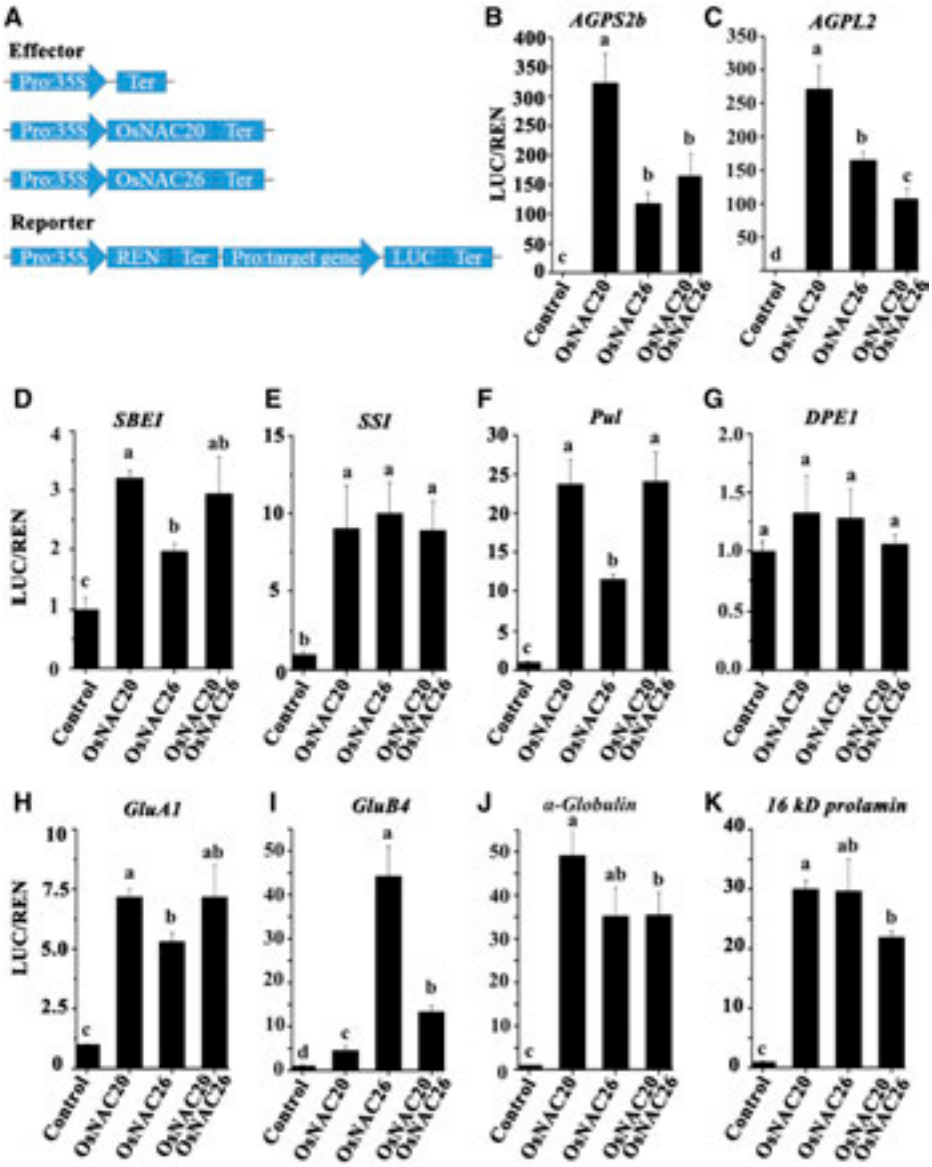

Figure 6. OsNAC20 and OsNAC26 stimulate the expression of starch and storage protein-related genes. A, Schematic diagram of the effector and reporter vectors for dual-luc assays. LUC, Firefly luciferase; REN, Renilla luciferase; Ter, Terminator. B to K, Relative luciferase activity was examined in *N. benthamiana* leaves cotransfected with the reporter and different effector constructs. A 1- to 3-kb region upstream of the start codon in these genes was selected as the gene promoter for firefly luciferase. Values are means ± SD from at least three biological replicates. Different lowercase letters indicate significant difference ($P < 0.05$) as determined by one-way ANOVA and Tukey's honestly significant difference (HSD) mean-separation test.

SBEI activity was complemented by SBEIIa and SBEIIb. We are inclined to favor the former hypothesis, as an extra SBEIIb activity has a remarkable effect on the molecular structure of starch (Tanaka et al., 2004), whereas the molecular structure and physicochemical properties of starch in the *osnac20/26-1* mutant were not significantly changed (Supplemental Fig. S9, C–E). In addition, SBEI can be phosphorylated (Tetlow et al., 2004; Qiu et al., 2016), a posttranslational modification that might keep its full enzyme activity in the double mutant, even if its mRNA and protein level are decreased. With regard to *DPE1*, although OsNAC20 and OsNAC26 could not directly bind to its promoter to regulate its expression (Fig. 6G), its RNA level, protein amount, and enzyme activity were significantly decreased (Fig. 5, B and F). This might be attributed to a physical/functional interaction of DPE1 with other starch synthetic enzymes, and therefore, it was reduced along with other components in the isozyme complex. Hwang et al. (2016) reported that Pho1 assembles with DPE1 to form a protein complex that enhances the synthesis of malto-oligosaccharides. However, Pho1 was not significantly different between cv ZH11 and the *osnac20/26-1* mutant. Therefore, this hypothesis might be impossible. More evidence is needed to demonstrate why *DPE1* was affected in this double mutant.

Generally, a decrease in starch content is accompanied by a change in starch morphology. In the *osnac20/26-1* mutant, starch showed a heterogeneous size, but it exhibited a polygonal shape (Supplemental Fig. S9, A and B). In addition, the amylose content in this double mutant was increased (Fig. 2K; Supplemental Fig. S9C; Supplemental Table S2). Previous reports have indicated that single mutations of *SSI* and *Pul* do not affect starch morphology and amylose content (Satoh et al., 2003; Fujita et al., 2006, 2009), whereas *DPE1* deficiency results in changes in starch morphology and increased amylose

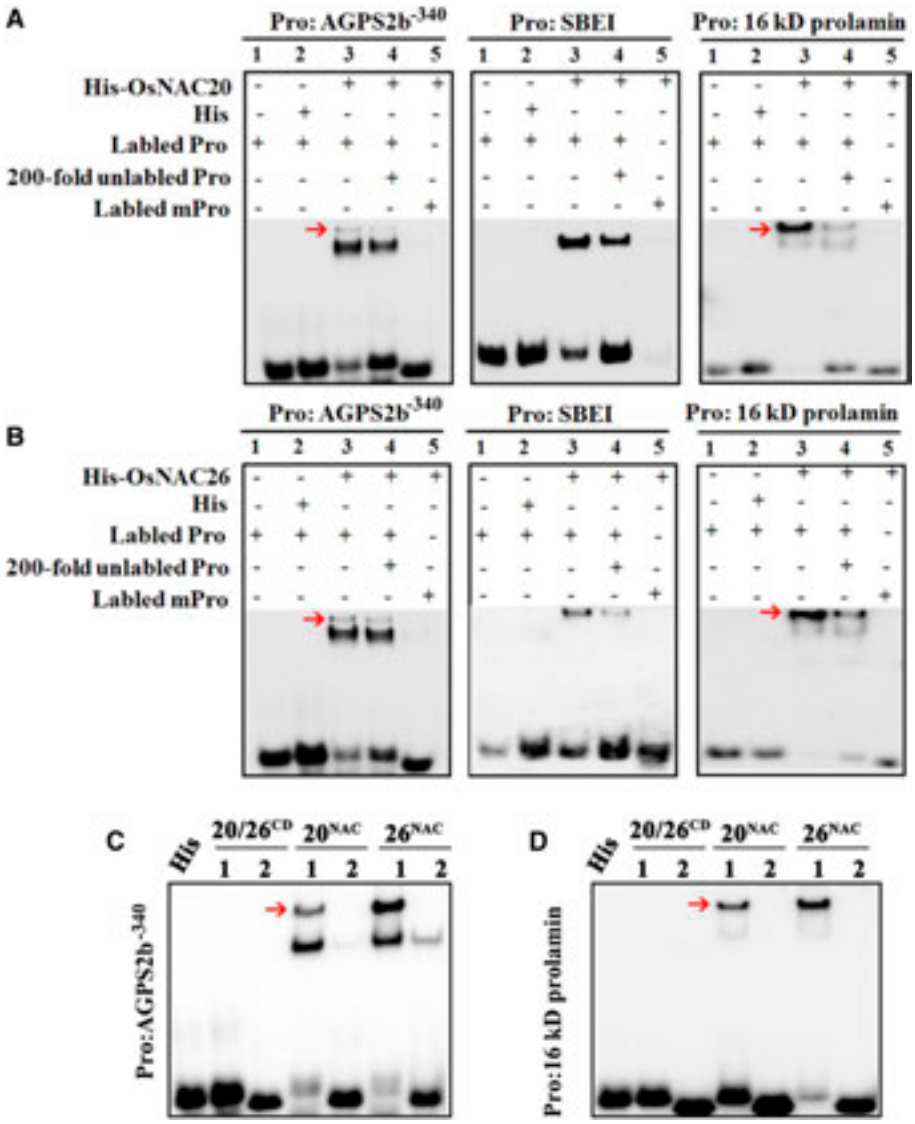

Figure 7. OsNAC20 and OsNAC26 directly bind to the promoters of *AGPS2b*, *SBEI*, and *16 kD prolamin*. A and B, EMSA of OsNAC20 (A) and OsNAC26 (B) with the promoters of starch and protein synthesis-related genes, respectively. Pro, Promoter; mPro, mutated promoter. Both His-OsNAC20 and His-OsNAC26 were able to bind to the promoters of *SBEI* and *16 kD prolamin* and induced a mobility shift (lane 3), while addition of an unlabeled probe competitively interacted with the recombinant proteins and resulted in a compromised band (lane 4). In addition, His and the mutated fragment alone did not cause this mobility shift (lanes 2 and 5, respectively). C, EMSA confirming the domain that interacts with the DNA sequence. $20/26^{CD}$ indicates the same subdomain C and D in OsNAC20 and OsNAC26 (Supplemental Fig. S1B). 20^{NAC} and 26^{NAC} represent the NAC domains in OsNAC20 and OsNAC26, respectively. Numbers 1 and 2 represent the probe and mutated probe, respectively. Probe sequences are listed in Supplemental Table S5. The red arrow indicates the positive band.

content, similar to those observed in the *osnac20/26-1* mutant (Dong et al., 2015), indicating that in the *osnac20/26-1* mutant, the slight changes in starch morphology and amylose content were caused by decreases in *DPE1* expression and activity. However, the starch content in *DPE1*-deficiency transgenic lines does not show a significant difference from that of the wild type (Dong et al., 2015). Therefore, it is concluded that the significantly decreased starch content in the *osnac20/26-1* mutant is a combined result of the reduced expression of *SSI*, *Pul*, and *DPEI*. In addition, Pul was decreased largely at RNA and enzyme activity levels, which implies that OsNAC20 and OsNAC26 are the main regulators for *Pul*.

OsNAC20 and OsNAC26 Regulate Storage Protein Synthesis

OsNAC20 and OsNAC26 directly bound to the promoters of *GluA1*, *GluB4*, *α-globulin*, and *16 kD prolamin* to regulate storage protein synthesis (Figs. 6 and 7). OsNAC20 and OsNAC26 deficiency caused an almost complete loss of *α*-globulin and 16 kD prolamin and severely decreased GluB4 (Fig. 5, H and I; Table 1); therefore, OsNAC20 and OsNAC26 are the main regulators for the three genes. The 16 kD prolamin protein is located in PBI, and its loss resulted in a pronounced decrease in PBI number and area (Fig. 4, C–F), indicating that 16 kD prolamin is required for PBI initiation and filling. A similar case in which prolamin is responsible for PB initiation has been reported in the maize 27-kD *γ*-zein protein, but 27-kD *γ*-zein is not required for the bulk of PB filling (Lopes and Larkins, 1995; Moro et al., 1995; Guo et al., 2013). GluA1, GluB4 and *α*-globulin are contained in PBII, and reduction of these proteins led to deficient filling of PBII.

We found that storage protein accumulation was not always mainly limited by its transcript amount. For example, GluA2, GluB1, GluB2, and

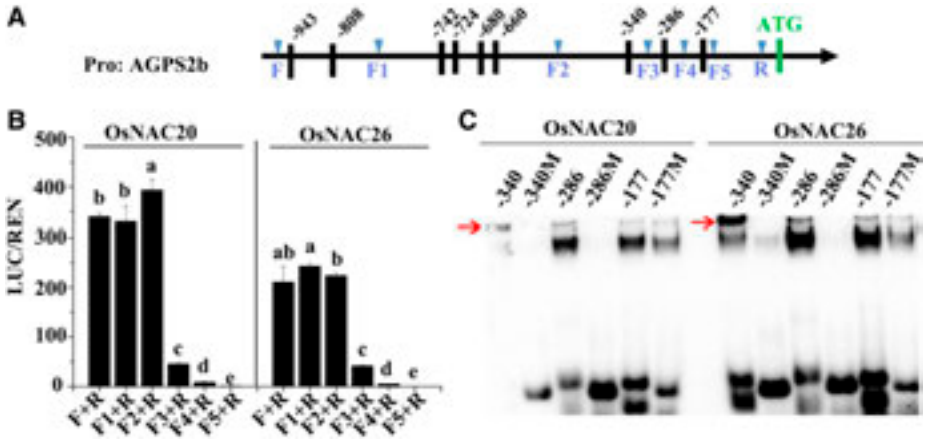

Figure 8. Identification of cis-elements targeted by OsNAC20 and OsNAC26 in the *AGPS2b* promoter. A, Schematic representation showing predicted NAC binding sites in the *AGPS2b* promoter. F to F5 and R represent the primers designed in the *AGPS2b* promoter. Black vertical bars represent the predicted NAC binding sites. Pro:AGPS2b, *APGS2b* promoter. B, Relative luciferase activity of different truncated *AGPS2b* promoters bound by OsNAC20 and OsNAC26. Values are means ± SD from at least three biological replicates. REN, Renilla luciferase; LUC, firefly luciferase. Different lowercase letters indicate significant difference ($P < 0.05$) as determined by one-way ANOVA and Tukey's honestly significant difference (HSD) mean-separation test. C, EMSA identifying binding activity of the three DNA fragments containing the −340, −266, and −177 binding sites with OsNAC20 and OsNAC26. The red arrow indicates the positive band. M, Mutated probe. Probe sequences are listed in Supplemental Table S5. The core binding sites were deleted in the mutated probes.

GluC transcripts were reduced to ~32%, 22%, 20%, and 16% of cv ZH11 levels, respectively, whereas their protein abundance was comparable to control levels (Fig. 5, H and I; Table 1; Supplemental Fig. S12C). Although GluA1 transcripts were dramatically decreased, the protein was not reduced to quite the same extent (Fig. 5H; Table 1). A similar phenomenon has also been reported in maize by other groups. Guo et al. (2013) observed that in 19- and 22-kD α-zein RNA interference transgenic plants, dramatic reduction of the transcripts of these two proteins does not result in a corresponding reduction of their protein abundance. Li et al. (2018b) found that in the *zmbzip22* mutant, an obvious transcript increase in 15-kD β-zein did not cause a noticeable increase in this zein at the protein level. This finding suggests that an excessive transcript level of storage protein, available amino acids, and translational machinery may also be responsible for storage protein abundance (Guo et al., 2013).

The expression of genes encoding major prolamins and globulin was decreased (Table 1), but the expression of *Os12g0269100*, *Os03g0766350*, and *Os05g0116000*, which encode minor prolamins and globulin, was increased (Supplemental Table S3). The supplementary expression of the three genes is promoted to counterbalance the deficit. (Kusaba et al., 2003; Kawakatsu et al., 2010; Lee et al., 2015). A similar protein rebalancing phenomenon has also been reported in other species, including barley (*Hordeum vulgare*; Hansen et al., 2007), rapeseed (*Brassica napus*; Rolletschek et al., 2020), wheat (Barro et al., 2016), soybean (*Glycine max*; Schmidt et al., 2011), and maize (Wu and Messing, 2014). However, the compensatory mechanism has not been identified.

OsNAC20 and OsNAC26 Are Redundantly Required for Starch and Storage Protein Synthesis

Three lines of evidence indicate that OsNAC20 and OsNAC26 have a redundant function in the regulation of starch and storage protein syntheses. First, OsNAC20 and OsNAC26 proteins share high similarity and they activate the same targets. They have almost identical NAC domains, except for three amino acid deletions in the NAC domain of OsNAC20, and their TRR domains share 76% sequence similarity (Supplemental Fig. S1). The NAC domain is responsible for cis-element interaction and the TRR domain contributes to its activation or repression properties (Ooka et al., 2003; Olsen et al., 2005). In this study, the NAC domains of OsNAC20 and OsNAC26 bind to the same cis-elements and activate the same starch and protein synthase-related genes (Figs. 6–8). Second, their promoters share 91% sequence similarity in that they have highly similar cis-elements in their promoters (Supplemental Table S6), meaning that *OsNAC20* and *OsNAC26* might have similar expression patterns. This is further demonstrated by the RT-qPCR result, which showed that both *OsNAC20* and *OsNAC26* are only detected at developing endosperm and both have their lowest and highest expression at 4 and 13 DAF, respectively (Fig. 1, A and B). Third, single mutation of *OsNAC20* and *OsNAC26* did not affect the grain phenotype, but simultaneous mutation of these two genes resulted in a floury grain phenotype (Fig. 2; Supplemental Figs. S7 and S8). The normal phenotype in

their respective single mutants is due to the increased expression level of the other *OsNAC* to compensate for the loss of function (Supplemental Fig. S14).

Several Other NAC TFs Might Take Part in Storage Product Accumulation

In RNA-seq data, we detected 8 other NAC TFs that changed their expression. *OsNAC25* (Os11g0512000), *OsNAC41* (Os01g0925400), *OsNAC128* (Os11g0512200), and *OsNAC129* (Os11g0512600) were downregulated in the endosperm of the *osnac20/26* mutant. *OsNAC25*, *OsNAC128*, and *OsNAC129* are endosperm-specific genes, and *OsNAC25* has a similar expression pattern to that of *OsNAC20* and *OsNAC26*. *OsNAC41* (Os01g0925400) is a candidate for high-yield genes in rice (Huang et al., 2018). These four NAC TFs might play a role in storage product accumulation, but how they take part in this process and how they are regulated by OsNAC20 and OsNAC26 are worth further investigation. Four stress-associated genes, *OsNAC2/OMTN2* (Os04g0460600), *OsNAC11/OMTN4* (Os06g0675600), *OsNAC39/OsCUC1* (Os03g0327100), and *OsNAC45* (Os11g0127600), were upregulated in the endosperm of the *osnac20/26* mutant (Fang et al., 2008, 2014; Zheng et al., 2009), which might contribute to the function of OsNAC20 and OsNAC26 in the stress response. In addition, their upregulation might be to compensate for the deficiency of OsNAC20 and OsNAC26 in the *osnac20/26* mutant.

In conclusion, OsNAC20 and OsNAC26 redundantly and directly transactivate the expression of *SSI*, *Pul*, *GluA1*, *GluB4/5*, *α-globulin*, and *16 kD prolamin* and indirectly influence *DPE1* expression to regulate starch and storage protein synthesis. These findings have also expanded our understanding of the NAC family in the regulation of endosperm starch and storage protein synthesis in plants.

MATERIALS AND METHODS

Plant Materials and Growth Conditions

The CRISPR/Cas9 constructs were generated in a *japonica* rice (*Oryza sativa*) 'Zhonghua11' (ZH11) background using a CRISPR/Cas9 Kit (Biogle) that contains CRISPR plasmids BGK032 (for the single mutant) and BGK032-DSG (for the double mutant). Briefly, for the single mutant, the synthesized target single guide RNA (sgRNA) sequences were inserted between the OsU6 promoter and the sgRNA scaffold by recombination reaction. For the double mutant, one target was inserted between the OsU6 promoter and the sgRNA and another between OsU3 and the sgRNA. The transgenic T1 to T4 plants were planted in the transgenic closed experiment field of Yangzhou University (Yangzhou, Jiangsu Province, China) under natural field conditions from May to September during the period 2016 to 2019. T3 plants and T4 grains were used for analysis in this study. In addition, the T3 plants used for follow-up seed phenotype observation were planted in Sanya (Hainan Province, China) from December 2017 to April 2018.

Protein Extraction, SDS-PAGE, and Immunoblot

The protein extraction for SDS-PAGE and immunoblot analysis of storage protein was conducted as described by Tian et al. (2013). All other protein samples were extracted as described previously (Wang et al., 2018). SDS-PAGE and immunoblot analyses were conducted according to the methods of Tian et al. (2013) and Wang et al. (2018). The starch synthesis- and storage protein synthesis-related antibodies were described previously (He et al., 2013; Liu et al., 2014).

Subcellular Localization Assays and Bimolecular Fluorescence Complementation

Both OsNAC20 and OsNAC26 were cloned into a 35S-GFP vector, 35S-1305, for subcellular localization analysis in *Nicotiana benthamiana* leaves. Both OsNAC20 and OsNAC26 were fused to pXY106 (nYFP-C) and pXY104 (N-cYFP) to observe their interactions in *N. benthamiana* leaves. The detailed transformation into the *Agrobacterium tumefaciens* strain and the infiltration into *N. benthamiana* leaves were performed as previously described (Cui et al., 2016). The primers used in this article are listed in Supplemental Table S7.

Immunofluorescence Analysis

The hulled grains at 8 DAF were fixed in phosphate buffer with paraformaldehyde and then embedded into paraffin. The samples were incubated with anti-OsNAC20 or anti-OsNAC26, followed by incubation with fluorescent secondary antibodies. The detailed immunofluorescence analysis was performed following the method of Wang et al. (2018).

Microscopic Observation

Semithin sections of developing and mature grains were investigated following the method of Zhao et al. (2016b). These sections were stained with iodine solution to observe starch granules, and stained with Coomassie brilliant blue and acid fuchsin to observe storage proteins. The stained sections were observed and photographed with a fluorescence microscope (BX51, Olympus). Transmission electron microscopy was conducted as described previously (Tian et al., 2013).

Pull-Down Assay

The CDSs of OsNAC20 and OsNAC26 were inserted into pET-32a and pGEX-6P-1 vectors, respectively. The empty and recombinant plasmids were transformed into *Escherichia coli* BL21 cells to express the fused protein, followed by protein purification using the corresponding beads. Glutahione *S*-transferase (GST)- or OsNAC26-GST coupled beads were used to capture His or OsNAC20-His and then their interaction was detected with anti-His antibodies.

Determination of Starch, Storage Protein, Amylose, and Soluble Sugar Contents and Starch M_r Distribution

The starch, storage protein, amylose, and soluble sugar contents were determined as described by Man et al. (2014) and Wang et al. (2018). The M_r distribution of starch was analyzed using gel-permeation chromatography described by Man et al. (2014).

Analyses of Thermal and Crystalline Properties

The thermal and crystalline properties of starch were investigated using differential scanning calorimetry and X-ray powder diffraction as described previously (Man et al., 2014).

Enzyme Activity Assay

Endosperm samples at 10 DAF were derived and homogenized on ice in extraction buffer (50 mM HEPES-NaOH [pH 7.4], 2 mM $MgCl_2$, and 12.5% [v/v] glycerol). The resulting supernatant was used for further enzyme activity analysis. Native PAGE/activity staining assays for DBE and SS were conducted following the method of Nishi et al. (2001). AGPase activity was recorded based on the amount of Glc-1-P produced by coupling its formation to NADH production using phosphoglucomutase and Glc-6-P dehydrogenase (Nishi et al., 2001). The detailed procedure was conducted using the ADPG Pyrophosphorylase Assay Kit (Solarbio). DPE1 assessment was based on a published

paper (Akdogan et al., 2011). Total SBE activity was measured using a SBE Assay Kit (Solarbio).

Transcriptome Analysis

Endosperm at 10 DAF was collected and used for RNA isolation with the Qiagen RNeasy mini kit. Paired-end libraries were synthesized through the TruSeq RNA Sample Preparation Kit (Illumina). Purified libraries were deep-sequenced using an Illumina HiSeq 2500. All sequencing raw data were pre-processed by filtering out other nonrelated reads and sequencing adapters and then mapped into the rice reference genome with two mismatches.

Dual-Luc Assay

Coding sequences of OsNAC20 and OsNAC26 were cloned into the 35S-1305 vector. The promoter sequences of starch synthesis- and storage protein synthesis-related genes were inserted into pGreenII-0080 vector. Then, all the recombinant vectors were transformed into Agrobacteria GV3101 or, in the case of the pGreenII-0080 constructs, cotransformed with pSoup-P19. The following procedures were conducted according to the method of Hellens et al. (2005). The activity of Renilla and LUC was determined using the Dual-Luciferase Reporter (DLR, Promega) and detected by BioTek Synergy2 (BioTek).

EMSA

The Web site http://plantpan2.itps.ncku.edu.tw/ was used to analyze the 1- to 3-kb upstream region of selected genes for the analysis of NAC protein binding sites. DNA fragments (30–50 bp) containing NAC protein biding sites were synthesized and labeled with the EMSA Probe Biotin Labeling Kit (Beyotime). The labeled probes were incubated with His-tagged OsNAC20 or OsNAC26 protein and then this mixture was run on an 8% (w/v) native polyacrylamide gel. After transferring to a nylon membrane, cross-linking, and blocking, the signal was detected with the Chemiluminescent EMSA Kit (Beyotime).

Statistical Analysis

The significance of intergroup differences was investigated by one-way ANOVA and Tukey's honestly significant difference (HSD) mean-separation test. Significance of difference between two groups of data was assessed by Student's *t* test.

Accession Numbers

Sequence data from this article can be found in the GenBank/EMBL data libraries under accession numbers OsNAC20 (LOC_Os01g01470), OsNAC26 (LOC_Os01g29840), AGPS2b (LOC_Os08g25734), AGPL2 (LOC_Os01g44220), SBEI (LOC_Os06g51084), SBEIIa (LOC_Os04g33460), SBEIIb (LOC_Os02g32660), Pho1 (Os04g0164900; LOC_Os03g55090), Pul (LOC_Os04g08270), GBSSI (LOC_Os06g04200), ISA1 (LOC_Os08g40930), SSI (LOC_Os06g06560), SSIIa (LOC_Os06g12450), SSIIIa (LOC_Os08g09230), DPE1 (LOC_Os07g43390), GluA1 (LOC_Os01g55690), GluA2 (LOC_Os10g26060), GluB1 (LOC_Os02g15178), GluB2 (LOC_Os02g15150), GluC (LOC_Os02g25640), 13 kD prolamin (LOC_Os07g10570), and 16 kD prolamin (LOC_Os06g31070).

Supplemental Data

The following supplemental materials are available.

Supplemental Figure S1. Alignment analysis of coding and amino acid sequences of OsNAC20 and OsNAC26.

Supplemental Figure S2. Primers for RT-qPCR and antigen sequence for anti-OsNAC20 and anti-OsNAC26.

Supplemental Figure S3. Subcellular localization of OsNAC20-eGFP and OsNAC26-eGFP in *N. benthamiana* leaves.

Supplemental Figure S4. Interaction assay between OsNAC20 and OsNAC26.

Supplemental Figure S5. Phylogenetic analysis of OsNAC20 and OsNAC26.

Supplemental Figure S6. Sequencing results of possible off-target matches.

Supplemental Figure S7. Grain phenotypic analysis of the *osnac20* and *osnac26* single mutants.

Supplemental Figure S8. A follow up phenotype observation in the *osnac20/26* mutant.

Supplemental Figure S9. Morphology, crystalline, and gelatinization properties of starch in cv ZH11 and *osnac20/26*.

Supplemental Figure S10. Storage protein phenotype analysis in endosperm of the *osnac20/26-1* mutant.

Supplemental Figure S11. Repeatability between three independent biological replicates of RNA-seq.

Supplemental Figure S12. RT-qPCR and immunoblot analysis of starch synthesis- and storage protein synthesis-related genes and protein expressions.

Supplemental Figure S13. The preharvest sprouting and fast germination phenomenon in seeds from the *osnac20/26* mutant.

Supplemental Figure S14. Relative expression levels of *OsNAC20* and *OsNAC26* in their respective single mutants.

Supplemental Table S1. Possible off-target matches.

Supplemental Table S2. M_r distribution of starch isolated from mature seeds.

Supplemental Table S3. Differentially expressed genes between cv ZH11 and the *osnac20/26-1* mutant.

Supplemental Table S4. Predicted NAC binding sites in the promoters of target genes.

Supplemental Table S5. DNA sequences for the EMSA in this article.

Supplemental Table S6. Predicted cis-elements in the *OsNAC20* and *OsNAC26* promoters.

Supplemental Table S7. Primers used in this article.

ACKNOWLEDGMENTS

We thank Xiuling Cai (Yangzhou University) and Ying He (Huazhong Agricultural University) for providing the antibodies for starch biosynthesis-related enzymes and storage protein synthesis-related protein, respectively. We thank Jianxiang Liu (Zhejiang University) for providing the dual-luc-related plasmids. We thank Dongping Zhang, Chen Chen, Baixiao Niu, Jian Wu, and Yijun Wang (Yangzhou University) for providing the advice about this research.

Received July 28, 2020; accepted September 16, 2020; published September 28, 2020.

LITERATURE CITED

Aida M, Ishida T, Fukaki H, Fujisawa H, Tasaka M (1997) Genes involved in organ separation in *Arabidopsis*: An analysis of the cup-shaped cotyledon mutant. Plant Cell **9:** 841–857

Akdogan G, Kubota J, Kubo A, Takaha T, Kitamura S (2011) Expression and characterization of rice disproportionating enzymes. J Appl Glycosci **58:** 99–105

Ascencio-Ibáñez JT, Sozzani R, Lee TJ, Chu TM, Wolfinger RD, Cella R, Hanley-Bowdoin L (2008) Global analysis of Arabidopsis gene expression uncovers a complex array of changes impacting pathogen response and cell cycle during *geminivirus* infection. Plant Physiol **148:** 436–454

Balazadeh S, Kwasniewski M, Caldana C, Mehrnia M, Zanor MI, Xue GP, Mueller-Roeber B (2011) ORS1, an H_2O_2-responsive NAC transcription factor, controls senescence in *Arabidopsis thaliana*. Mol Plant **4:** 346–360

Barro F, Iehisa JCM, Giménez MJ, García-Molina MD, Ozuna CV, Comino I, Sousa C, Gil-Humanes J (2016) Targeting of prolamins by RNAi in

bread wheat: Effectiveness of seven silencing-fragment combinations for obtaining lines devoid of coeliac disease epitopes from highly immunogenic gliadins. Plant Biotechnol J **14:** 986–996

Beckles DM, Smith AM, ap Rees T (2001) A cytosolic ADP-glucose pyrophosphorylase is a feature of graminaceous endosperms, but not of other starch-storing organs. Plant Physiol **125:** 818–827

Bello BK, Hou Y, Zhao J, Jiao G, Wu Y, Li Z, Wang Y, Tong X, Wang W, Yuan W, et al (2019) NF-YB1-YC12-bHLH144 complex directly activates *Wx* to regulate grain quality in rice (*Oryza sativa* L.). Plant Biotechnol J **17:** 1222–1235

Cai XL, Xie DL, Wang ZY, Hong MM (2002) Interaction of rice bZIP protein REB with the 5′-upstream region of both rice *sbe1* gene and *waxy* gene. Chin Sci Bull **47:** 310–314

Chen J, Yi Q, Cao Y, Wei B, Zheng L, Xiao Q, Xie Y, Gu Y, Li Y, Huang H, et al (2016) ZmbZIP91 regulates expression of starch synthesis-related genes by binding to ACTCAT elements in their promoters. J Exp Bot **67:** 1327–1338

Cord Neto G, Yunes JA, da Silva MJ, Vettore AL, Arruda P, Leite A (1995) The involvement of Opaque 2 on β-prolamin gene regulation in maize and *Coix* suggests a more general role for this transcriptional activator. Plant Mol Biol **27:** 1015–1029

Cui J, You C, Zhu E, Huang Q, Ma H, Chang F (2016) Feedback regulation of DYT1 by interactions with downstream bHLH factors promotes DYT1 nuclear localization and anther development. Plant Cell **28:** 1078–1093

Davis JP, Supatcharee N, Khandelwal RL, Chibbar RN (2003) Synthesis of novel starches *in planta*: Opportunities and challenges. Starch **55:** 107–120

Denyer KAY, Johnson P, Zeeman S, Smith AM (2001) The control of amylose synthesis. J Plant Physiol **158:** 479–487

Dong J, Zheng Y, Fu Y, Wang J, Yuan S, Wang Y, Zhu Q, Ou X, Li G, Kang G (2019b) PDIL1-2 can indirectly and negatively regulate expression of the AGPL1 gene in bread wheat. Biol Res **52:** 56

Dong Q, Wang F, Kong J, Xu Q, Li T, Chen L, Chen H, Jiang H, Li C, Cheng B (2019a) Functional analysis of *ZmMADS1a* reveals its role in regulating starch biosynthesis in maize endosperm. Sci Rep **9:** 3253

Dong X, Zhang D, Liu J, Liu QQ, Liu H, Tian L, Jiang L, Qu Q (2015) Plastidial disproportionating enzyme participates in starch synthesis in rice endosperm by transferring maltooligosyl groups from amylose and amylopectin to amylopectin. Plant Physiol **169:** 2496–2512

Fang Y, Xie K, Xiong L (2014) Conserved miR164-targeted NAC genes negatively regulate drought resistance in rice. J Exp Bot **65:** 2119–2135

Fang Y, You J, Xie K, Xie W, Xiong L (2008) Systematic sequence analysis and identification of tissue-specific or stress-responsive genes of NAC transcription factor family in rice. Mol Genet Genomics **280:** 547–563

Feng F, Qi W, Lv Y, Yan S, Xu L, Yang W, Yuan Y, Chen Y, Zhao H, Song R (2018) OPAQUE11 is a central hub of the regulatory network for maize endosperm development and nutrient metabolism. Plant Cell **30:** 375–396

Ferrero DML, Piattoni CV, Asencion Diez MD, Rojas BE, Hartman MD, Ballicora MA, Iglesias AA (2020) Phosphorylation of ADP-glucose pyrophosphorylase during wheat seeds development. Front Plant Sci **11:** 1058

Fu F-F, Xue H-W (2010) Coexpression analysis identifies Rice Starch Regulator1, a rice AP2/EREBP family transcription factor, as a novel rice starch biosynthesis regulator. Plant Physiol **154:** 927–938

Fujita N, Toyosawa Y, Utsumi Y, Higuchi T, Hanashiro I, Ikegami A, Akuzawa S, Yoshida M, Mori A, Inomata K, et al (2009) Characterization of pullulanase (PUL)-deficient mutants of rice (*Oryza sativa* L.) and the function of PUL on starch biosynthesis in the developing rice endosperm. J Exp Bot **60:** 1009–1023

Fujita N, Yoshida M, Asakura N, Ohdan T, Miyao A, Hirochika H, Nakamura Y (2006) Function and characterization of starch synthase I using mutants in rice. Plant Physiol **140:** 1070–1084

Giroux MJ, Hannah LC (1994) ADP-glucose pyrophosphorylase in *shrunken-2* and *brittle-2* mutants of maize. Mol Gen Genet **243:** 400–408

Guo X, Yuan L, Chen H, Sato SJ, Clemente TE, Holding DR (2013) Non-redundant function of zeins and their correct stoichiometric ratio drive protein body formation in maize endosperm. Plant Physiol **162:** 1359–1369

Hansen M, Lange M, Friis C, Dionisio G, Holm PB, Vincze E (2007) Antisense-mediated suppression of C-hordein biosynthesis in the barley grain results in correlated changes in the transcriptome, protein profile, and amino acid composition. J Exp Bot **58:** 3987–3995

He Y, Wang S, Ding Y (2013) Identification of novel glutelin subunits and a comparison of glutelin composition between *japonica* and *indica* rice (*Oryza sativa* L.). J Cereal Sci **57:** 362–371

Hellens RP, Allan AC, Friel EN, Bolitho K, Grafton K, Templeton MD, Karunairetnam S, Gleave AP, Laing WA (2005) Transient expression vectors for functional genomics, quantification of promoter activity and RNA silencing in plants. Plant Methods **1:** 13

Huang H, Xie S, Xiao Q, Wei B, Zheng L, Wang Y, Cao Y, Zhang X, Long T, Li Y, et al (2016) Sucrose and ABA regulate starch biosynthesis in maize through a novel transcription factor, *ZmEREB156*. Sci Rep **6:** 27590

Huang J, Li J, Zhou J, Wang L, Yang S, Hurst LD, Li WH, Tian D (2018) Identifying a large number of high-yield genes in rice by pedigree analysis, whole-genome sequencing, and CRISPR-Cas9 gene knockout. Proc Natl Acad Sci USA **115:** E7559–E7567

Hwang SK, Koper K, Satoh H, Okita TW (2016) Rice endosperm starch phosphorylase (Pho1) assembles with disproportionating enzyme (Dpe1) to form a protein complex that enhances synthesis of malto-oligosaccharides. J Biol Chem **291:** 19994–20007

Kawakatsu T, Hirose S, Yasuda H, Takaiwa F (2010) Reducing rice seed storage protein accumulation leads to changes in nutrient quality and storage organelle formation. Plant Physiol **154:** 1842–1854

Kawakatsu T, Yamamoto MP, Touno SM, Yasuda H, Takaiwa F (2009) Compensation and interaction between RISBZ1 and RPBF during grain filling in rice. Plant J **59:** 908–920

Kim JS, Chae S, Jun KM, Pahk YM, Lee TH, Chung PJ, Kim YK, Nahm BH (2017) Genome-wide identification of grain filling genes regulated by the OsSMF1 transcription factor in rice. Rice (N Y) **10:** 16

Kubo M, Udagawa M, Nishikubo N, Horiguchi G, Yamaguchi M, Ito J, Mimura T, Fukuda H, Demura T (2005) Transcription switches for protoxylem and metaxylem vessel formation. Genes Dev **19:** 1855–1860

Kusaba M, Miyahara K, Iida S, Fukuoka H, Takano T, Sassa H, Nishimura M, Nishio T (2003) Low glutelin content1: A dominant mutation that suppresses the glutelin multigene family via RNA silencing in rice. Plant Cell **15:** 1455–1467

Lee HJ, Jo YM, Lee JY, Lim SH, Kim YM (2015) Lack of globulin synthesis during seed development alters accumulation of seed storage proteins in rice. Int J Mol Sci **16:** 14717–14736

Li C, Qiao Z, Qi W, Wang Q, Yuan Y, Yang X, Tang Y, Mei B, Lv Y, Zhao H, et al (2015) Genome-wide characterization of *cis*-acting DNA targets reveals the transcriptional regulatory framework of *Opaque2* in maize. Plant Cell **27:** 532–545

Li C, Yue Y, Chen H, Qi W, Song R (2018a) The ZmbZIP22 transcription factor regulates 27-kD γ-zein gene transcription during maize endosperm development. Plant Cell **30:** 2402–2424

Li X, Chang Y, Ma S, Shen J, Hu H, Xiong L (2019) Genome-wideidentification of SNAC1-targeted genes involved in drought response in rice. Front Plant Sci **10:** 1–14

Li Y, Yu G, Lv Y, Long T, Li P, Hu Y, Liu H, Zhang J, Liu Y, Li WC, et al (2018b) Combinatorial interaction of two adjacent *cis*-active promoter regions mediates the synergistic induction of *Bt2* gene by sucrose and ABA in maize endosperm. Plant Sci **274:** 332–340

Liu D, Wang W, Cai X (2014) Modulation of amylose content by structure-based modification of OsGBSS1 activity in rice (*Oryza sativa* L.). Plant Biotechnol J **12:** 1297–1307

Lopes MA, Larkins BA (1995) Genetic analysis of *opaque2* modifier gene activity in maize endosperm. Theor Appl Genet **91:** 274–281

Man J, Lin L, Wang Z, Wang Y, Liu Q, Wei C (2014) Different structures of heterogeneous starch granules from high-amylose rice. J Agric Food Chem **62:** 11254–11263

Mao C, Lu S, Lv B, Zhang B, Shen J, He J, Luo L, Xi D, Chen X, Ming F (2017) A rice NAC transcription factor promotes leaf senescence via ABA biosynthesis. Plant Physiol **174:** 1747–1763

Mathew IE, Das S, Mahto A, Agarwal P (2016) Three rice NAC transcription factors heteromerize and are associated with seed size. Front Plant Sci **7:** 1638

Moro GL, Lopes MA, Habben JE, Hamaker BR, Larkins BA (1995) Phenotypic effects of *opaque2* modifier genes in normal maize endosperm. Cereal Chem **72:** 94–99

Nakamura Y (2002) Towards a better understanding of the metabolic system for amylopectin biosynthesis in plants: Rice endosperm as a model tissue. Plant Cell Physiol **43:** 718–725

Nie DM, Ouyang YD, Wang X, Zhou W, Hu CG, Yao J (2013) Genome-wide analysis of endosperm-specific genes in rice. Gene **530:** 236–247

Nishi A, Nakamura Y, Tanaka N, Satoh H (2001) Biochemical and genetic analysis of the effects of amylose-extender mutation in rice endosperm. Plant Physiol **127:** 459–472

Olsen AN, Ernst HA, Leggio LL, Skriver K (2005) NAC transcription factors: Structurally distinct, functionally diverse. Trends Plant Sci **10:** 79–87

Ooka H, Satoh K, Doi K, Nagata T, Otomo Y, Murakami K, Matsubara K, Osato N, Kawai J, Carninci P, et al (2003) Comprehensive analysis of NAC family genes in *Oryza sativa* and *Arabidopsis thaliana*. DNA Res **10:** 239–247

Peng X, Wang Q, Wang Y, Cheng B, Zhao Y, Zhu S (2019) A maize NAC transcription factor, *ZmNAC34*, negatively regulates starch synthesis in rice. Plant Cell Rep **38:** 1473–1484

Qiao Z, Qi W, Wang Q, Feng Y, Yang Q, Zhang N, Wang S, Tang Y, Song R (2016) ZmMADS47 regulates zein genetranscription through interaction with Opaque2. PLoS Genet **12:** e1005991

Qiu J, Hou Y, Tong X, Wang Y, Lin H, Liu Q, Zhang W, Li Z, Nallamilli BR, Zhang J (2016) Quantitative phosphoproteomic analysis of early seed development in rice (*Oryza sativa* L.). Plant Mol Biol **90:** 249–265

Rolletschek H, Schwender J, König C, Chapman KD, Romsdahl T, Lorenz C, Braun HP, Denolf P, Van Audenhove K, Munz E, et al (2020) Cellular plasticity in response to suppression of storage proteins in the *Brassica napus* embryo. Plant Cell **32:** 2383–2401

Saito Y, Shigemitsu T, Yamasaki R, Sasou A, Goto F, Kishida K, Kuroda M, Tanaka K, Morita S, Satoh S, et al (2012) Formation mechanism of the internal structure of type I protein bodies in rice endosperm: Relationship between the localization of prolamin species and the expression of individual genes. Plant J **70:** 1043–1055

Sakuraba Y, Kim D, Han SH, Kim SH, Piao W, Yanagisawa S, An G, Paek NC (2020) Multilayered regulation of membrane-bound ONAC054 is essential for abscisic acid-induced leaf senescence in rice. Plant Cell **32:** 630–649

Satoh H, Nishi A, Yamashita K, Takemoto Y, Tanaka Y, Hosaka Y, Sakurai A, Fujita N, Nakamura Y (2003) Starch-branching enzyme I-deficient mutation specifically affects the structure and properties of starch in rice endosperm. Plant Physiol **133:** 1111–1121

Satoh H, Shibahara K, Tokunaga T, Nishi A, Tasaki M, Hwang S-K, Okita TW, Kaneko N, Fujita N, Yoshida M, et al (2008) Mutation of the plastidial α-glucan phosphorylase gene in rice affects the synthesis and structure of starch in the endosperm. Plant Cell **20:** 1833–1849

Schmidt MA, Barbazuk WB, Sandford M, May G, Song Z, Zhou W, Nikolau BJ, Herman EM (2011) Silencing of soybean seed storage proteins results in a rebalanced protein composition preserving seed protein content without major collateral changes in the metabolome and transcriptome. Plant Physiol **156:** 330–345

Song Y, Luo G, Shen L, Yu K, Yang W, Li X, Sun J, Zhan K, Cui D, Liu D, et al (2020) *TubZIP28*, a novel bZIP family transcription factor from *Triticum urartu*, and *TabZIP28*, its homologue from *Triticum aestivum*, enhance starch synthesis in wheat. New Phytol **226:** 1384–1398

Souer E, van Houwelingen A, Kloos D, Mol J, Koes R (1996) The *no apical meristem* gene of Petunia is required for pattern formation in embryos and flowers and is expressed at meristem and primordia boundaries. Cell **85:** 159–170

Sun D, Zhang X, Zhang Q, Ji X, Jia Y, Wang H, Niu L, Zhang Y (2019) Comparative transcriptome profiling uncovers a *Lilium regale* NAC transcription factor, *LrNAC35*, contributing to defence response against cucumber mosaic virus and tobacco mosaic virus. Mol Plant Pathol **20:** 1662–1681

Tanaka N, Fujita N, Nishi A, Satoh H, Hosaka Y, Ugaki M, Kawasaki S, Nakamura Y (2004) The structure of starch can be manipulated by changing the expression levels of starch branching enzyme IIb in rice endosperm. Plant Biotechnol J **2:** 507–516

Tetlow IJ (2006) Understanding storage starch biosynthesis in plants: A means to quality improvement. Can J Bot **84:** 1167–1185

Tetlow IJ, Wait R, Lu Z, Akkasaeng R, Bowsher CG, Esposito S, Kosar-Hashemi B, Morell MK, Emes MJ (2004) Protein phosphorylation in amyloplasts regulates starch branching enzyme activity and protein-protein interactions. Plant Cell **16:** 694–708

Tian L, Dai LL, Yin ZJ, Fukuda M, Kumamaru T, Dong XB, Xu XP, Qu Q (2013) Small GTPase Sar1 is crucial for proglutelin and α-globulin export from the endoplasmic reticulum in rice endosperm. J Exp Bot **64:** 2831–2845

Tuncel A, Kawaguchi J, Ihara Y, Matsusaka H, Nishi A, Nakamura T, Kuhara S, Hirakawa H, Nakamura Y, Cakir B, et al (2014) The rice endosperm ADP-glucose pyrophosphorylase large subunit is essential for optimal catalysis and allosteric regulation of the heterotetrameric enzyme. Plant Cell Physiol **55:** 1169–1183

Vicente-Carbajosa J, Moose SP, Parsons RL, Schmidt RJ (1997) A maize zinc-finger protein binds the prolamin box in zein gene promoters and interacts with the basic leucine zipper transcriptional activator Opaque2. Proc Natl Acad Sci USA **94:** 7685–7690

Wang J, Hu P, Lin L, Chen Z, Liu Q, Wei C (2018) Gradually decreasing starch branching enzyme expression is responsible for the formation of heterogeneous starch granules. Plant Physiol **176:** 582–595

Wang JC, Xu H, Zhu Y, Liu QQ, Cai XL (2013) OsbZIP58, a basic leucine zipper transcription factor, regulates starch biosynthesis in rice endosperm. J Exp Bot **64:** 3453–3466

Wang X, Culver JN (2012) DNA binding specificity of ATAF2, a NAC domain transcription factor targeted for degradation by *Tobacco mosaic virus*. BMC Plant Biol **12:** 157

Washida H, Wu CY, Suzuki A, Yamanouchi U, Akihama T, Harada K, Takaiwa F (1999) Identification of cis-regulatory elements required for endosperm expression of the rice storage protein glutelin gene *GluB-1*. Plant Mol Biol **40:** 1–12

Wu A, Allu AD, Garapati P, Siddiqui H, Dortay H, Zanor M-I, Asensi-Fabado MA, Munné-Bosch S, Antonio C, Tohge T, et al (2012) JUNGBRUNNEN1, a reactive oxygen species-responsive NAC transcription factor, regulates longevity in *Arabidopsis*. Plant Cell **24:** 482–506

Wu C, Washida H, Onodera Y, Harada K, Takaiwa F (2000) Quantitative nature of the Prolamin-box, ACGT and AACA motifs in a rice glutelin gene promoter: Minimal *cis*-element requirements for endosperm-specific gene expression. Plant J **23:** 415–421

Wu Y, Messing J (2014) Proteome balancing of the maize seed for higher nutritional value. Front Plant Sci **5:** 240

Wu Y, Messing J (2012) Rapid divergence of prolamin gene promoters of maize after gene amplification and dispersal. Genetics **192:** 507–519

Yamagata H, Sugimoto T, Tanaka K, Kasai Z (1982) Biosynthesis of storage proteins in developing rice seeds. Plant Physiol **70:** 1094–1100

Yamaguchi M, Kubo M, Fukuda H, Demura T (2008) Vascular-related NAC-DOMAIN7 is involved in the differentiation of all types of xylem vessels in Arabidopsis roots and shoots. Plant J **55:** 652–664

Yamamoto MP, Onodera Y, Touno SM, Takaiwa F (2006) Synergism between RPBF Dof and RISBZ1 bZIP activators in the regulation of rice seed expression genes. Plant Physiol **141:** 1694–1707

Yano M, Isono Y, Satoh H, Omura T (1984) Gene analysis of sugary and shrunken mutants of rice, *Oryza sativa* L. Jpn J Breeding **34:** 43–49

Zhang D, Zhang M, Zhou Y, Wang Y, Shen J, Chen H, Zhang L, Lü B, Liang G, Liang J (2019a) The rice G protein γ subunit DEP1/qPE9–1 positively regulates grain-filling process by increasing auxin and cytokinin content in rice grains. Rice (N Y) **12:** 91

Zhang J, Chen J, Yi Q, Hu Y, Liu H, Liu Y, Huang Y (2014) Novel role of ZmaNAC36 in co-expression of starch synthetic genes in maize endosperm. Plant Mol Biol **84:** 359–369

Zhang Z, Dong J, Ji C, Wu Y, Messing J (2019b) NAC-type transcription factors regulate accumulation of starch and protein in maize seeds. Proc Natl Acad Sci USA **116:** 11223–11228

Zhang Z, Yang J, Wu Y (2015) Transcriptional regulation of zein gene expression in maize through the additive and synergistic action of Opaque2, Prolamine-box binding factor, and O2 heterodimerizing proteins. Plant Cell **27:** 1162–1172

Zhang Z, Zheng X, Yang J, Messing J, Wu Y (2016) Maize endosperm-specific transcription factors O2 and PBF network the regulation of protein and starch synthesis. Proc Natl Acad Sci USA **113:** 10842–10847

Zhao F, Ma J, Li L, Fan S, Guo Y, Song M, Wei H, Pang C, Yu S (2016a) GhNAC12, a neutral candidate gene, leads to early aging in cotton (*Gossypium hirsutum* L). Gene **576:** 268–274

Zhao L, Pan T, Cai C, Wang J, Wei C (2016b) Application of whole sections of mature cereal seeds to visualize the morphology of endosperm cell and starch and the distribution of storage protein. J Cereal Sci **71:** 19–27

Zheng X, Chen B, Lu G, Han B (2009) Overexpression of a NAC transcription factor enhances rice drought and salt tolerance. Biochem Biophys Res Commun **379:** 985–989